MINISTRY OF EDUCATION AND SCIENCE OF UKRAINE
NATIONAL TECHNICAL UNIVERSITY OF UKRAINE
"IGOR SIKORSKY KYIV POLYTECHNIC INSTITUTE"

E.O. Paton Educational and Scientific Institute of

Materials Science and Welding

Department of Physical Materials Science and Heat Treatment

«On the rights of the manuscript»
УДК 539.264

"Admitted to defense"
Head of the department
_____Myroslav KARPETS
«16» грудня 2022

Master's thesis

for a master's degree
in the specialty 132 Materials Science

on the topic: «The effect of mechanical processing of a mixture 80% Al_2O_3/20% Fe_2O_3 powders on the structure and electrochemical properties of lithium current sources»

Completed by:
2nd-year student of the group ФМ-11мп
Liu GUANNAN _____
Supervisor
PhD., Ass. prof., Associate Professor
Yurii YAVORSKYI _____
Consultants:
labor protection and safety in emergency situations
Dr.Sci., prof., Head of the department
Oleh LEVCHENKO _____
the economic and organizational section:
PhD, Ass. prof., Associate Professor,
Serhii NARAYEVSKYI _____
Norm control:
PhD, Ass. prof., Associate Professor
Vadym KHRYSTENKO _____
Reviewer:
Dr.Sci., Ass. prof., Professor
Anatolii MINITSKYI _____

I certify that in this master's dissertation there are no borrowings from the works of other authors without proper references.
Student _____

Kyiv – year 2022

MINISTRY OF EDUCATION AND SCIENCE OF UKRAINE
NATIONAL TECHNICAL UNIVERSITY OF UKRAINE
"IGOR SIKORSKY KYIV POLYTECHNIC INSTITUTE"

E.O. Paton Educational and Scientific Institute of

Materials Science and Welding

Department of Physical Materials Science and Heat Treatment

The second level (master's) of higher education according to the educational-professional program

Specialty - 132 "Materials Science"

Specialization - "Materials science and computer modeling of heat treatment processess"

APPROVE

«Admission to the defence»

Head of the department

_____Myroslav KARPETS

«___ »_____2022 .

TASK

for a master's thesis of a student

Liu Guannan

1. Dissertation topic "The effect of mechanical processing of a mixture of 80% Al_2O_3/20% Fe_2O_3 powders on the structure and electrochemical properties of lithium current sources", scientific supervisor of the dissertation is PhD, Assoc. Prof. Yurii Yavorskyi are approved by the order of the University of 9 November 2022p. № 4129-c

2. The deadline for students to submit a dissertation is December 16.12.2022p.

3. Object of study: a Al_2O_3/20% Fe_2O_3 mixture

4. Output data: SEM and TEM images, XRD data, O$K\alpha$-, Fe$L\alpha$- and Al$L\alpha$- specters, data of galvanostatic analysis

5. List of tasks to be performed: literature review, research methodology, experiment results and discussion, organizational and economic part, labor protection, designing a master's thesis.

6. Approximate list of graphic (illustrative) material:SEM images, X-ray diffraction maps of mixtures, X-ray diagrams.

7. Approximate list of publications:

1) Y. V. Yavorskyi, Ya. V. Zaulychnyy, O. I. Dudkaa, Liu Guannan / Effect of machining time on the electronic structure of 20%Al_2O_3/80% SiO_2 / VII Всеукраїнської науково-практичної конференції здобувачів вищої освіти та молодих вчених «Фізика і хімія твердого тіла. Стан, досягнення і перспективи» / Луцьк, Україна, 21-22 жовтня 202. – ст. 134-135.

2) Тези МТО

8. Consultants of the Dissertation sections

Section	Surname, initials and position consultant	Signature, date	
		Task issued	Task accepted
Occupational health and safety in emergencies	Dr.Sci., prof., Head of the department Oleh LEVCHENKO		
Economic and organizational section	PhD, Ass. prof., Associate Professor, Serhii NARAYEVSKYI		
Norm control	PhD, Ass. prof., Associate Professor Vadym KHRYSTENKO		

9. The date of issuance of the task is 1 September 2021p.

CALENDAR SCHEDULE OF THE PRACTICE

№	The name of the stages of the thesis	The term of performance of work stages	Note
1	Acquaintance with the equipment of the department and methodology of envistigation	07.09.2022	***Done***
2	Conducting a literature review on research topics	21.09.2022	***Done***
3	Analyzing SEM research results	28.09.2022	***Done***
4	Analyzing the results of X-ray structural studie	05.10.2022	***Done***
5	Analyzing the results of an ultra-soft X-ray emission study	12.10.2022	***Done***
6	Analyzing the results of galvanostatic cycling	19.10.2022	***Done***
7	Writing a pre-diploma practice report	26.10.2022	***Done***

Student _____ Liu Guannan

Supervisor _____ Yurii Yavorskyi

ABSTRACT

Explanatory note: 87 pages, 21 figures, 23 tables, 55 sources.

The object of the study – the structural and electrochamical charcteristics of the powder mixture 80% Al_2O_3/20% Fe_2O_3.

The aim of the work is to investigate the influence of mechanoactivations on the morphology and electrochemical properties of 80% Al_2O_3/20% Fe_2O_3 nanocomposite.

Methods of research: Ultra-soft X-ray emission spectroscopy, X-ray diffraction analysis, raster and transmission electronic microscopy, galvanostatic analysis.

Modern technology requires the creation of new materials with the best electro-chemical and operational properties that meet the criteria of manufacturability, environmental friendliness, low cost. Therefore, the study of the properties of materials with unique features is undoubtedly relevant. This master thesis presents the study of influence of mechanoactivation Al_2O_3 and α-Fe_2O_3 mixture with a component ratio of 80/20% on the structure and electrochemical characteristics.

From the results of investigation established that the charging capacity of the LPS with a cathode based on the mechanoactivated mixture increases due to the injection of Al_2O_3 nanoparticles into α-Fe_2O_3 nanoparticles and the increase in surface defects of the nanocomposite.

FERUM OXIDE, ALUMINUM OXIDE, SHOCK VIBRATION TREATMENT, MORPHOLOGY, ULTRA-SOFT X-RAY EMISSION SPECTROSCOPY, ELECTROCHEMISTRY.

АНОТАЦІЯ

Пояснювальна записка: 87 стор., 21 рис., 23 таблиці, 55 джерел.

Об’єкт дослідження – структурні та електрохімічні характеристики суміші порошків 80% Al_2O_3/20%.

Метою роботи є дослідження впливу механоактивації на структуру та електрохімічні властивості нанокомпозиту 80% Al_2O_3/20% Fe_2O_3.

Методи дослідження: ультрам'яка рентгенівська емісійна спектроскопія, рентгеноструктурний аналіз, растрова електронна мікроскопія, трансмісійна електронна мікроскопія, гальваностатичний аналіз.

Сучасні технології вимагають створення нових матеріалів з найкращими електрохімічними та експлуатаційними властивостями, що відповідають критеріям технологічності, екологічності, дешевизни. Тому вивчення властивостей матеріалів з унікальними властивостями є безсумнівно актуальним. У цій роботі представлено дослідження впливу механоактивації суміші Al_2O_3 та α-Fe_2O_3 із співвідношенням компонентів 80/20% на структуру та електрохімічні властивості.

Отриманими в роботі результатами встановлено, що зарядна ємність ЛПС з катодом на основі механоактивованої суміші підвищується за рахунок вколювання наночастинок Al_2O_3 в частинки α-Fe_2O_3 та збільшення поверхневих дефектів нанокопмозиту.

ОКСИД ФЕРУМУ, ОКСИД АЛЮМІНІЮ, УДАРНО-ВІБРАЦІЙНА ОБРОБКА, МОРФОЛОГІЯ, УЛЬТРАМ'ЯКА РЕНТГЕНОВСЬКА ЕМІСІЙНА СПЕКТРОСКОПІЯ, ЕЛЕКТРОХІМІЯ.

CONTENT

CHAPTER 1. LITERATURE REVIEW

1.1. Description of nanosized aluminum oxide

1.1.1. Manufacturing methods

There are many preparation methods for high-purity nano-alumina powder, which can be roughly divided into solid phase method, liquid phase method, gas phase method, etc. Various methods have certain advantages, but there are also shortcomings, so generally different preparation methods are selected according to the actual product requirements.

Mechanochemical method. The mechanochemical method is the solid-phase reaction of aluminum powder and other metal oxides under ball milling conditions to generate alumina powder. By ball milling ZnO and aluminum, ZnO and aluminum undergo solid-phase reaction, ZnO is reduced to Zn, and aluminum is oxidized to Al_2O_3, thereby obtaining 10~50nm amorphous alumina particles [1]. The temperature required for this reaction is much lower than that of the combustion reaction, and the reaction can be controlled stepwise in a lower temperature environment, so it can be used in the preparation of anti-corrosion, anti-wear coatings and metal-templated composite reinforcements.

Plasma method. The plasma method mainly heats the gas to turn it into a plasma gas, and then reacts the aluminum salt with the air in the plasma gas atmosphere, and finally the quenched product condenses into tiny particles, and the generated alumina product can be on the wall of the reaction vessel collect [2]. The main advantage of the plasma method is that the high temperature of the plasma and the high enthalpy of the reaction can make the less reactive species react. Additionally, the quench step promotes uniform nucleation, which is beneficial for the formation of nanoparticles. C-Al_2O_3 powders with a particle size distribution of several to 30 nm were prepared by the thermal plasma method, using argon and nitrogen as plasma gases to react pressurized air and aluminum powders [3].

Sol-gel method. In the sol-gel method, organic alkoxides or inorganic salts are uniformly distributed in the liquid phase to form a sol, and then water is added to

make it react to form a gel under certain conditions such as temperature and pH value. After the gel is dried, it is calcined at different temperatures to obtain the desired powder [4]. The advantage of the sol-gel method is that the reaction is carried out at room temperature and the reaction conditions are controllable. But the cost is high and there is a certain amount of environmental pollution.

Precipitation method. $Al(OH)_3$ is an amphoteric oxide, which can promote the reaction of Al^{3+} in solution to form $Al(OH)_3$ precipitation by adjusting the pH. For some soluble aluminum salts, such as $AlCl_3$, $Al(NO_3)$, etc., the precipitation of $Al(OH)_3$ can be produced by adding alkaline substances to adjust the pH value of the solution. Alumina can be obtained by heat treatment of $Al(OH)_3$ [5]. This preparation process is relatively simple and the production cost is low, but the particle size is not easy to control, and other methods need to be used for auxiliary improvement.

Aluminium ammonium sulfate pyrolysis method. Aluminium ammonium sulfate pyrolysis method is a preparation method for obtaining alumina powder by heating and decomposing ammonium aluminium sulfate. It has been reported that A-Al_2O_3 with an average particle size of 25 nm can be obtained by modification with polyethylene glycol. The pyrolysis method of aluminum ammonium sulfate can be used in large-scale production, but harmful gases such as SO_2 appear in the reaction, which will cause environmental pollution [6].

$$2NH_4A1(SO_4)_2 \cdot 12H_20 — A1_20_3+2NH_3+4S0_2+13H_20$$

Pyrolysis of aluminum ammonium carbonate. The ammonium aluminum carbonate is heated and decomposed, and the powder is then phase-inverted and pulverized to obtain high-purity ultra-fine alumina powder. In fact, this method is an improvement to the situation that ammonium aluminum sulfate decomposes and emits harmful gas SO_2 in the pyrolysis of ammonium aluminum sulfate. The key to this method is to obtain high-purity basic ammonium aluminum carbonate. For example, first prepared the precursor $NH_4Al(OH)_2CO_3$ by homogeneous precipitation, and then heated and decomposed $NH_3Al(OH)_2CO_2$ to obtain alumina nanoparticles [7]. Uses ammonium aluminum carbonate pyrolysis to obtain alumina of 40-50 nm,

and sinters alumina at 1450-1500□, which greatly reduces the sintering temperature.

Alkoxide hydrolysis. Alkoxide hydrolysis is a method in which the desired product is obtained by the decomposition of an alkoxide in water. Alkoxide hydrolysis is one of the methods for preparing various ultrafine oxide powders. Generally speaking, metal alkoxides are soluble in organic solvents, and are easily decomposed into corresponding oxides or hydrated oxides when exposed to water. By adjusting various parameters and surfactants of the glass and enamel solution system, nanoparticles with different morphologies and particle size distributions can be obtained.The preparation of Al_2O_3 by alkoxide hydrolysis will obtain different products due to different conditions, not only can obtain AlO (OH) amorphous and crystalline powder, but also can obtain transparent sol. Usually ethanol or isopropanol is used as the solvent. Since the alkoxide hydrolysis product is the same as the solvent, it can be reused and the production cost can be reduced [8][9]**.**

Improvement of the sol-gel method. The preparation of alumina powder by sol-gel method has its own disadvantages. If an aluminum salt (eg. $A1C1_3$) is used as a raw material, corrosive gas may be generated during the reaction process and the later calcination process. However, if organic alkoxides are used, problems such as high cost of raw materials and difficult storage due to strong activity will be faced. In order to solve the above problems, Thiruchitrambalama et al.[10] used direct hydrolysis of metal aluminum, and dispersed the product into a sol by ultrasonic vibration and other methods, and then evaporated the water to form a boehmite (boehmite) gel. Finally, alumina is obtained by calcining at 1000□ for 1 h, which is much lower than the 1200□required for directly calcining boehmite to generate alumina. Due to the high specific surface energy of nanoparticles, it is easy to agglomerate. Nanoscale particles that are uniformly dispersed in the liquid phase process will agglomerate due to drying in air. Therefore, special drying methods are required to eliminate the gas-liquid interface, thereby reducing the occurrence of agglomeration. Chen Haiyang et al. used a combination of sol-gel method and supercritical drying to prepare nano-alumina powder. Through supercritical drying, the uniformly dispersed hydrated alumina sol was less likely to agglomerate during

the drying process. Supercritical drying method can be used to obtain alumina ultrafine particles with large specific surface, large average pore size and high pore volume [11]. The shape of alumina ultrafine particles is fibrous particles with a length of 100 nm and a diameter of about 10 nm, and the particle distribution is relatively uniform.

Solution combustion decomposition method. The solution combustion decomposition method is a preparation method of using a salt solution to add a combustion agent to carry out a combustion reaction, thereby obtaining the required powder. The heat released by the method during combustion can promote the formation of single-phase substances. In addition [12], the raw materials used in this method come from a wide range of sources and the cost is relatively low added citric acid and ammonia to the $A1(NO)_3$, aqueous solution, adjusted the pH value of the solution with ammonia water and dilute nitric acid, then evaporated the solution to make it undergo a combustion reaction to obtain sponge-like aluminum hydroxide, and then obtained by calcination Alumina,. Studies have shown that the pH of the initial solution has a great influence on the final shape of the alumina particles. When the initial solution Ph=2, the reaction is slow, and the final powder is flake-like, the particle size is greater than lm, and the thickness is about 200nm. However, when pH=10, the reaction is faster, and alumina particles with a narrow distribution and a particle size of several hundreds of nanometers are generated.

Liquid phase flame jet pyrolysis. The liquid phase flame jet pyrolysis method uses different precursors, chelates and surfactants, which are fully mixed and ignited by oxygen spray, thereby obtaining the desired oxide or hydroxide. T. Hinklin et al [13]. adopted this method, using different precursors such as aluminum nitrate and aluminum acetylacetonate [$A1_{(Acac)}$] to dissolve in a mixture of ethanol and tetrahydrofuran, and then spray and mix with oxygen to ignite to prepare nano-alumina. Among them, the use of inorganic salts $A1C_{13}$ and $A1(NO_3)_3$ can only obtain alumina particles with larger particle size and pores. However, using $Al_{(Acac)}$, an alumina powder of less than 20 nm was obtained with a specific surface area of 60 m2/g. Since the surface of the obtained powder is highly carboxylated, this nano-

alumina may be suitable for making catalyst supports or making ceramic materials.

Nanoparticle induction method. Incorporating nano-scale alumina powder into the system for preparing alumina powder by wet method is helpful for the growth of nanoparticles, and at the same time, the temperature for forming alumina can be reduced, and the occurrence of alumina particles caused by high temperature can be effectively controlled [14]. added 2% (molar ratio) of spherical nano-alumina with an average particle size of 100 nm in the precipitation process, and finally obtained a disc-shaped alumina with a particle length of 300 nm and a width of 80 nm, and the transition temperature of the α phase was down to 1100□. Kanichi Kamiya et al [15]. added 1% (mass) nano-alumina particles to the aluminum sec-butoxide-ethanol-hydrochloric acid-water system, so that 50% of the alumina was converted into nano-alumina at 600□.

1.1.2. Crystalline structure

Hexagonal unit cell. After analysis, the Al^{3+} layer and the oxygen ion layer are alternately arranged until the 13th layer until the repetition occurs, as shown in the following Figure for the hexagonal unit cell, Example reference to Figure 1.1 and Figure.1.2.

.

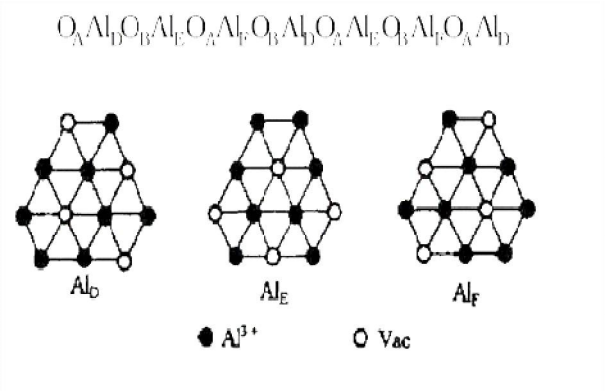

Figure 1.1. Hexagonal structure of aluminum oxide

Since Al^{3+} is in the gap of oxygen ions, only 2/3 of the gap is filled with Al^{3+}, and the remaining 1/3 of the gap is empty. Therefore, the distribution of Al^{3+} must

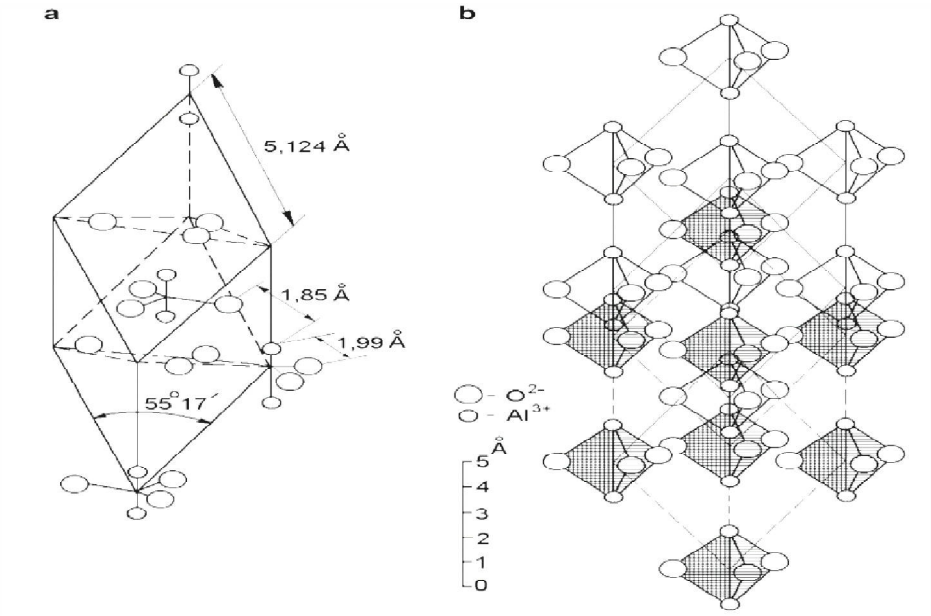

have a certain law, the original then is in the same layer and between layers, the distance between Al^{3+} should be kept the farthest.

Figure 1.2. Hexagonal unit cell of aluminum oxide

Rhombohedral unit cell 2 molecules per unit cell, i.e. 10 ions, 6 Al^{3+} and 4 O^{2-} Example for Figure.1.3.

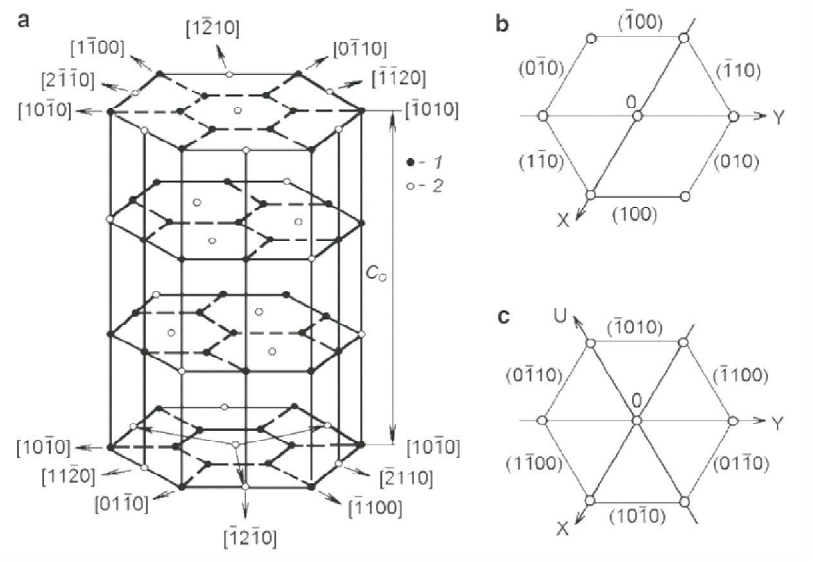

Figure 1.3. Rhombohedral unit cell of aluminum oxide

Octahedral element Each aluminum ion is surrounded by 6 oxygen ions, forming a twisted octahedron. Example reference to Figure.1.4.

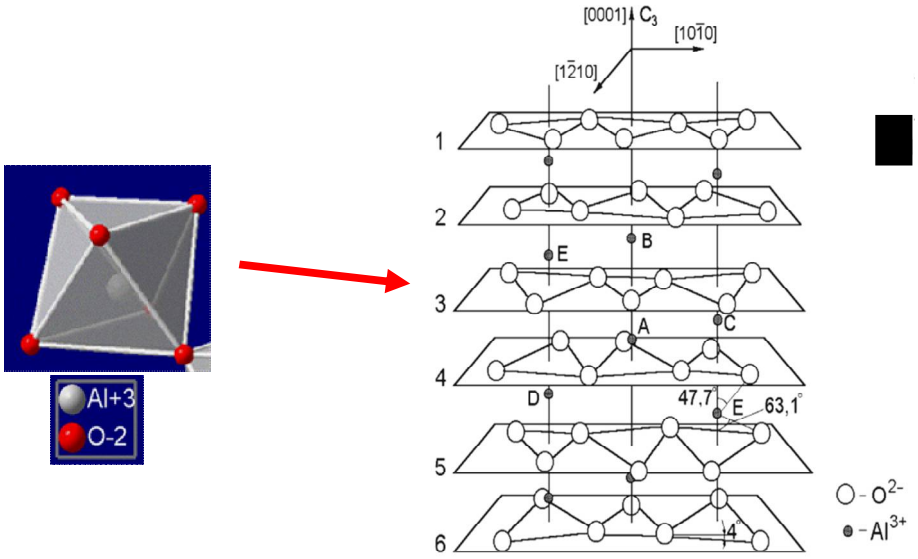

Figure 1.4. Octahedral element of aluminum oxide

1.1.3. Electronic structure

The energy band structure of a material describes the energy with which electrons are allowed or forbidden, which is caused by the diffraction of electron waves and determines many properties of the material, especially electrical and optical properties. Band structure is a common information obtained by first-principles calculations, which can help us understand the properties of materials more clearly, and provide an effective means for us to rationally explain metals, semiconductors, and insulators.

It is well known that grain boundaries, which form an important component of the microstructure of polycrystalline materials, have a pervasive influence on a variety of macroscopic properties and phenomena. In α-Al_2O_3, it has been shown that

the sintering, diffusion, deformation behaviour and segregation, as well as chemical and electrical properties, are sensitively dependent on the structure, composition and properties of grain boundaries [16].

The density of states of alumina consists of three regions, two valence bands and one conduction band. The lower energy region at the bottom of the valence band—19ev~16ev, the density of states is mainly composed of 2s orbitals of Al atoms and O atoms, and a few 3p orbitals from Al atoms. The upper part of the valence band is a bonding orbital between 6.8ev and 0.2ev, and its density of states is mainly composed of the 3p orbital of the Al atom and the 2p orbital of the O atom. The conduction band is mainly composed of 3p and 3s orbitals of Al and a few 2p orbitals of 0 atoms between 5ev and 15ev [17]. There is a certain degree of hybridization between the orbitals, but the hybridization is weak, forming part of covalent bonds.

1.1.4. Different types of morphology

Aluminum hydroxide is completely dehydrated at high temperature into a stable final product α-Al_2O_3. Before that, many different crystal forms can be formed due to differences in temperature, pressure, and vapor partial pressure. These crystal forms can be regarded as intermediate [or transition] form. At present, there are 8 kinds of Al_2O_3 crystal forms. Due to their different crystal transformation temperatures, alumina is divided into low temperature type and high temperature type. Alumina has been identified as α, β, γ, θ, κ, η, ρ, χ and so on. Chief among them are γ-alumina and α-alumina.(See Table 1.1)

Table 1.1. Properties of various crystal types

type		α	κ	θ	δ	χ	η	γ	ρ
		Al_2O_3							
structure		Hexagon	Hexagon	monoclinic	Quartet	Hexagon	Hexagon	Quartet	
density/g. cm^{-3}		3. 98	3. 1–3. 3	3. 4–3. 9	3. 2	3. 0	2. 5–3. 6	3. 2	
parameters ×10^{-10}m	a	4. 758	9. 71	11. 24	7. 94	5. 56	7. 92	8. 01	
	b			5. 72	7. 94				
	c	12. 991	17. 86	11. 74	23. 5	13. 44			

α-Al_2O_3 is the only crystal form that exists in nature,commonly known as corundum. Natural corundum generallycontains trace element impurities, mainly chromium,titanium, etc., and thus have different colors.The crystalform of corundum is often barrel-shaped, column-shaped or plate-shaped, and the crystal shape is mostly complete and vitreous. α-Al_2O_3 belongs to the hexagonal crystal system, and the oxygen ions are arranged in a hexagonal close-packed arrangement, that is, ABAB… two-layer repeating type. There are 4 aluminum ions entering the gap in each unit cell. The Figure below shows the octahedral gap formed by the close packing of oxygen ions in the α-Al_2O_3 structure by aluminum ions. O^{2-} is arranged in a hexagonal close-packed manner, Al^{3+} is in the gap of oxygen ions, at the center of an octahedron, but only 2/3 of the gap is filled with Al^{3+}.(See Figure 1.5)

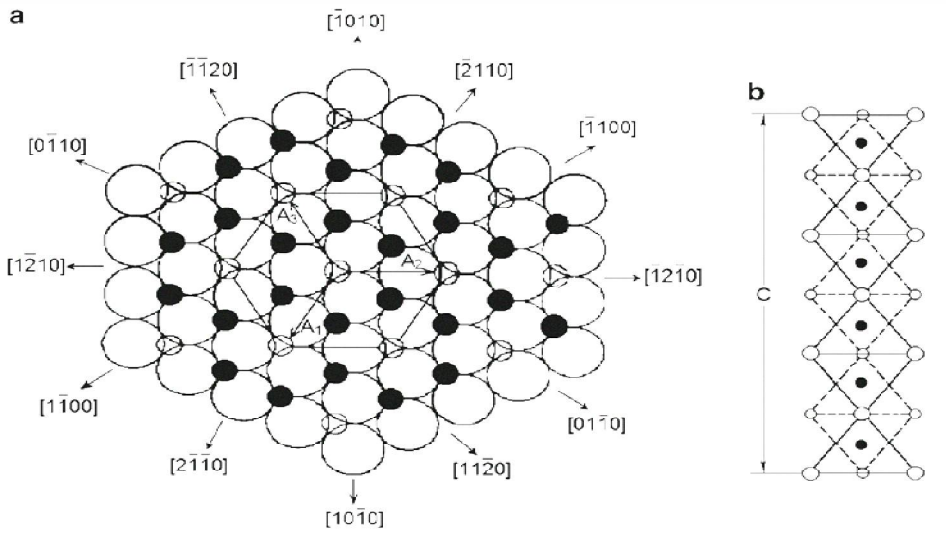

Figure 1.5. Crystal structure of α-Al2O3

β-Al_2O_3. β−Al_2O_3 is a high content of polyaluminate minerals, it is not a pure alumina, its chemical composition can be approximated by MeO-6 Al_2O_3 and Me_2O-11Al_2O_3 (MeO refers to CaO, BaO, SrO and other alkaline earth metals oxides; Me_2O refers to Na_2O, K_2O, Li_2O). β−Al_2O_3 (Me_2O-11Al_2O_3) is formed by overlapping stacking of [NaO]-layers and $[Al_{11}O_{12}]^+$ type spinel units, oxygen ions are arranged in cubic close packing, and sodium ions are completely contained in the [NaO]-layer plane, and can spread quickly. Under the right conditions, it has high ionic conductivity, so it is widely used in the production of electronic watches, electronic

cameras, stethoscopes and pacemakers.

γ-Al_2O_3. γ− Al_2O_3 is the most common transitional alumina, which belongs to the cubic crystal system and has a spinel structure, which does not exist in nature. Cubic close packing is formed by oxygen ions, and Al^{3+} fills in the gaps. γ−Al_2O_3 has a density of 3.42-3.62g/cm3, and can be slowly transformed into α-Al_2O_3 at 1000°C, which is a transitional alumina substance produced by gibbsite (Al_2O_3·H2O or Al_2O·3H2O) or aluminum hydroxide during heating. The main use of γ-phase particles is as a catalyst carrier. At present, trace elements such as rare earth elements are added to the γ-phase to improve its surface energy, thereby effectively inhibiting the occurrence of phase transformation and sintering, thereby improving the stability of the specific surface of the material. performance.

1.1.5. The use of Al_2O_3 as an electrode material for lithium current sources

Nano-alumina for lithium batteries is a nano-powder with small and uniform particle size, high purity and excellent surface performance produced by special processing technology according to the performance of batteries and battery materials. It is widely used in various lithium batteries, alkali It can improve the energy storage performance and safety performance of the battery, and play a role in energy saving and environmental protection.

Nano-alumina is used as an electrode coating for lithium batteries, which has the properties of insulation, heat insulation and high temperature resistance; as the capacity of lithium-ion rechargeable batteries continues to increase, the internal energy accumulated is increasing, and the internal temperature will increase. It is possible that the temperature is too high to melt the negative electrode separator and cause a short circuit; if a nano-alumina coating is applied to the separator, short circuit between electrodes can be avoided and the safety of lithium batteries can be improved.

Coating lithium cobalt oxide with nano-alumina, the nano-thick Al_2O_3 coating will greatly reduce the interface impedance, provide an additional electron transport

tunnel, greatly prevent the erosion of the electrolyte on the electrode, and can accommodate particles The volume change during Li^+ deintercalation prevents damage to the electrode structure.

The doping of aluminum ions in nano-alumina can increase the voltage of the battery, thereby improving the safety of the battery.

Nano-alumina is used for the battery film. With the continuous improvement of the capacity of lithium-ion rechargeable batteries, the energy accumulated inside will become larger and larger, and the internal temperature will increase. It is possible that the temperature is too high to melt the negative electrode diaphragm and cause a short circuit; if coating a layer of nano-alumina coating on the separator can avoid short circuit between electrodes and improve the safety of lithium battery.

During the charging and discharging process of lithium-ion batteries, lithium ions are repeatedly intercalated and deintercalated in the positive and negative electrode materials, so that the structure of the $LiCoO_2$ active material changes after multiple contractions and expansions, and at the same time, the $LiCoO_2$ interlayer loosens and falls off. The internal resistance increases and the electrochemical specific capacity decreases. Coating a layer of Al_2O_3 on the surface of $LiCoO_2$ can avoid the direct contact between $LiCoO_2$ and the electrolyte and reduce the loss of electrochemical specific capacity, thereby increasing the electrochemical specific capacity of $LiCoO_2$, improving its cycle performance and prolonging its service life.

1.2. Description of nanosized iron oxide

1.2.1. Manufacturing methods

At present, there are many different preparation methods of nano iron oxide at home and abroad, which can be generally divided into liquid phase method, solid phase method and gas phase method. The liquid phase method mostly uses $Fe(NO3)_3 \cdot 9H_2O$ or $FeCl_3 \cdot 6H_2O$ as raw material, and is prepared by precipitation hydrolysis method, sol-gel method, hydrothermal method, etc. The solid phase method mainly includes mechanical grinding method, solid phase reaction method or

Thermal decomposition and other methods; the gas phase method is a method of directly using gas or changing substances into gases by various means, making them undergo physical changes or chemical reactions in the gas state, and finally condensing and growing to form nanoparticles during the cooling process. There are preparation methods such as chemical vapor deposition (PCVD) and laser thermal decomposition.

Liquid phase method. Precipitation hydrolysis methodThe precipitation hydrolysis method is the earliest method used to synthesize metal oxide nanoparticles by liquid-phase chemical reaction.[18] The main process consists of two stages:(1) hydrolysis: $Fe^{3+} + 3(OH)^{-} \rightarrow Fe(OH)_3 + 3H^{+}$ (2) roasting: $Fe(OH)_3 \rightarrow Fe_2O_3$ According to the different processes, it can be divided into uniform hydrolysis method, forced hydrolysis method and microwave induced hydrolysis method [19].

Sol-gel method. Nano-sized iron oxide particles are prepared by the sol-gel method, mostly using high-valent iron salts such as $Fe(NO3)_3 \cdot 9H_2O$ or $FeCl_3 \cdot 6H_2O$ as the initial raw material, and at a certain temperature, with a lower than theoretical amount of alkali (such as NaOH) with it. Reaction to prepare $Fe(OH)_3$ sol [20]. Then add anionic surfactant (such as sodium dodecylbenzenesulfonate) to form an organic layer on the surface of the colloid and have hydrophobicity; use organic solvent (such as toluene, chloroform) for extraction, The $Fe(OH)_3$ sol was transferred to the organic phase, and the organic phase was distilled off under reduced pressure; the residue was heated to obtain nano iron oxide particles [21]. The equipment of the sol-gel method is relatively simple, the prepared nanoparticles are uniform and the particle size is relatively small, but the process parameters are strict and difficult to control, and toxic organic compounds will be volatilized during the preparation process, polluting the environment.

Hydrothermal method. Hydrothermal synthesis method refers to a synthesis method in which the original mixture is reacted in a closed system, using water as a solvent, at a certain temperature and the autogenous pressure of water. The hydrothermal synthesis method of nano-iron oxide mostly uses $Fe(NO_3)_3$ or $FeCl_3$ as raw materials [22]. First, $Fe(OH)_3$ gel is prepared. After redispersing with water, it is

added to the reaction kettle, and the temperature is raised to a certain temperature to react for a period of time. After cooling out of the kettle, it can be obtained by drying treatment.

Solid phase method. The mechanical pulverization method uses a stirring ball mill, a sand mill, a planetary ball mill, and the like. It is to put the material into the pulverizer and rely on the action of mechanical force to refine the material. The solid-phase chemical reaction method is to fully mix $Fe(NO_3)_3 \cdot 9H_2O$ or $FeCl_3 \cdot 6H_2O$ with NaOH according to a certain proportion, and then sinter, because the diffusion in the solid-phase reaction is very slow, and amorphous FeOOH is formed first, and the surface is coated. With NaCl, etc. to prevent it from continuing to grow or agglomerate, nano-scale particles can be obtained. Jing Su et al [23]. used FeCl3·6H2O and KOH as raw materials, and sintered them at a temperature of 600-800□ to obtain α-Fe_2O_3 of 40-50 nm. The solid-phase chemical reaction method has the advantages of simple operation, high conversion rate, less pollution, small particle size of the prepared product, uniform particle size distribution, and no agglomeration phenomenon.

Gas phase method. The gas phase method is a method of directly using gas or changing substances into gases by various means, making them undergo physical changes or chemical reactions in the gas state, and finally condensing and growing to form nanoparticles during the cooling process [24].

1.2.2. Electronic structure

The energy band structure of a material describes the energy with which electrons are allowed or forbidden, which is caused by the diffraction of electron waves and determines many properties of the material, especially electrical and optical properties.

Articles by Bertoncello et al , so in all the clusters investigated we assumed that each Fe and O atom contributes fifive (Fe^{3+}) and eight (O^{2-}) electrons, respectively. As a matter of fact, in a cluster of 33 atoms including 15 Fe centres, the

number of 3d Fe is quite large (5 × 15 × 2 = 150 the two is due to the spin-polarized treatment [25]) and the relative cluster MOs are very closely spaced.

1.2.3. Crystalline structure

Generally, iron oxides and their oxyhydroxides belong to the iron oxide series compounds, which can be divided into different valence states, crystal forms and structures α-, β-, γ-Fe_2O_3, Fe_3O_4, FeO and α-, β-, γ-, δ-FeOOH, According to the color, it can be divided into red, yellow, orange, brown, black and so on. The more practical ones are α-Fe_2O_3, γ-Fe_2O_3, α-FeOOH, Fe_3O_4.

Iron oxide, in particular, has many different phases, with Fe in variable oxidation states, depending upon the reduction process. The iron oxides include hematite (α-Fe_2O_3), magnetite (Fe_3O_4), and wustite (FeO). Fe_2O_3 exhibits various polymorphs including α-Fe_2O_3 (rhombohedral), γ-Fe_2O_3 (cubic), β-Fe_2O_3 (cubic), and ε-Fe_2O_3 (orthorhombic), among which α-Fe_2O_3 is the most thermodynamically stable phase. Both γ-Fe_2O_3 (space group: P4132, a = b = c = 0.8347 nm) and Fe_3O_4 (space group: Fd-3m, a = b = c = 0.8394 nm) share the cubic structure with close-packed oxygen atoms along the <111>direction but vary in the oxidation state for Fe ,9-10 Magnetite contains both Fe2+ and Fe3+ ionsin the crystal lattice and is sometimes formulated as $FeO{\cdot}Fe_2O_3$. In the crystal structure of Fe_3O_4, half of the Fe^{3+} ions are located in the tetrahedral interstitial sites, and the other half of the Fe3+ ions and all the Fe^{2+} ions occupy the octahedral sites. 11 In γ-Fe_2O_3, due to the absence of Fe^{2+}, some of the Fe positions are left unoccupied as random vacancies. FeO adopts the cubic, rock-salt structure, where Fe^{2+} ions are octahedrally coordinated by O^{2-} ions. The applications for iron oxides intimately depend on their ability to redox (reduction and oxidation) cycle between the +2 and +3 oxidation states. However, the variable oxidation states of iron lead to a fairly complicated phase diagram of iron oxides with several easily interchangeable phases (Figure.1.6.).

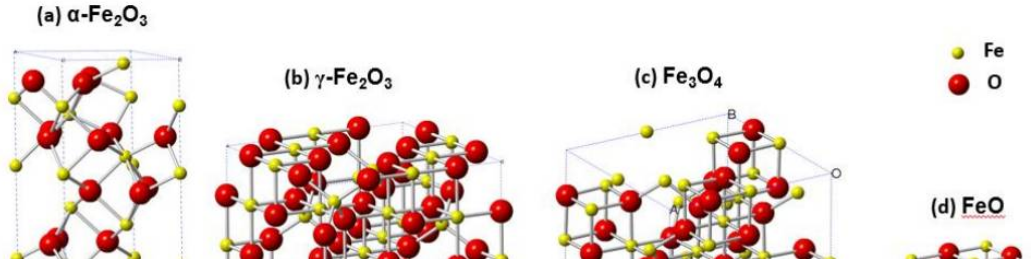

Figure 1.6. Crystal structures of various iron oxides

1.2.4. Different types of morphology

Fe_2O_3 has various crystal forms. Among the predominant α and γ-configured iron oxides, iron has a six-coordinated octahedral structure. That is, each iron center is complexed with six oxygens.

α crystal form. α-Fe_2O_3 has a rhombohedral crystal form and a corundum (α-Al_2O_3) structure, which is the most common crystal form. In nature, it exists in the form of hematite, the main iron ore. It is antiferromagnetic below about 260 K (the Morin phase transition temperature) and exhibits weak ferromagnetism between the Neel temperatures of 260 K and 950 K. Iron oxide can be easily prepared by thermal decomposition and liquid phase precipitation. Its magnetic properties depend on many factors, such as pressure, particle size, and magnetic field strength.

γ crystal form. γ-Fe_2O_3 has a cubic structure, which is slightly less stable and is transformed from α crystal form at high temperature. It occurs naturally in the form of the mineral maghemite, and usually ultrafine particles smaller than 10 nanometers in size are superparamagnetic, but it is ferromagnetic, which can be used on audio tapes. It can be prepared by heating and dehydration of γ-iron oxyhydroxide, and another method includes the controlled oxidation of ferric tetroxide. Ultrafine powder of γ-iron oxide can be prepared by thermal decomposition of iron (iii) oxalate.

Other crystal forms. Several other crystal forms were also confirmed. The β crystal form has a cubic nucleus (space group Ia3), is metastable, and converts to the α crystal form above 500°C. It can be prepared by carbon reduction of hematite, pyrolysis of ferric chloride solution or ferric sulfate. The ε crystal form is a

rhombohedral crystal form with properties intermediate between the α crystal form and the γ crystal form, and may have useful magnetic characteristics. Due to the contamination of the α crystal form and the γ crystal form, the preparation of pure ε crystal form iron oxide is very difficult. γ-iron oxide can prepare high content of ε-iron oxide material by thermal conversion. This crystalline form is also metastable, transforming to the alpha form between 500 and 750°C. The crystalline form of iron oxide can also be prepared by arc iron oxidation or by sol-gel precipitation from iron (III) nitrate. In addition, amorphous iron oxides have also been found under high pressure conditions.

1.2.5. The use of Fe_2O_3 as an electrode material for lithium current sources

The anode materials of lithium-ion batteries, such as iron oxide, have excellent electrochemical properties. Nano-sized iron oxide can reveal the transport distance of lithium ions, enhance the charging and discharging dynamics and has a large Capacitance value [26].

Application in lithium battery: Nano iron oxide is the main component of lithium iron phosphate battery, non-toxic, non-polluting, wide source of raw materials, low price, long life, etc. It has excellent cycle performance, high temperature resistance and safety performance. Compared with lead-acid batteries, lithium-ion batteries using iron oxide materials have increased driving distance, increased power, and increased speed.

During the charging process of Fe_2O_3 anode material, lithium ions will pass through the electrolyte and the separator to intercalate Fe_2O_3 to form Lix Fe_2O_3, and as the reaction progresses, Fe and Li_2O will finally be formed. The lithium discharge process corresponds to the extraction of lithium ions. At the same time, iron is also gradually oxidized from 0-valent iron to 3-valent iron ions, and finally forms Fe_2O_3. The lithium storage mechanism of Fe_2O_3 is simply that, when lithium intercalates, lithium ions combine with oxygen in Fe_2O_3 to form Li_2O. When delithiation is performed, Li_2O is reduced to lithium ions, and Fe_2O_3 is also formed again. During this process, the electrode material will undergo a large volume change, and even

lead to severe damage to the electrode, resulting in rapid capacity decay and affecting the battery's cycle performance. Therefore, researchers designed different types of nanostructured Fe_2O_3 or composited Fe_2O_3 particles with different types of carbon additives to improve the electrochemical performance.

1.3 Description of the Fe_2O_3/Al_2O_3 mixture

1.3.1. Mixture manufacturing methods and structure

The use of mechanical methods to mix in proportion is the most common preparation method. Here is a process of solution method.

Depending on a certain percentage, the nitrate, glycine, and carbon source are dissolved in ion water to form a solution: heating preparation solution, volatilization, concentrated and decomposing solution The heat treatment is performed to obtain iron oxide powder. The percentage percentage of the concentration of preparing iron oxide suspension is 20 %: add iron oxide powder to an absolute ethanol, and the ultrasonic dispersion is obtained to obtain iron oxide suspension; Methylbhenyate solution and continue to stir to obtain iron oxide hydroxide and iron oxide; ultrasonic dispersion and dry sintering to obtain 20 % iron oxide-80 % aluminum nanomantic material. The method in the above example has lower roughness and high polishing rate [27].

1.3.2. Use of lithium current sources as electrode material

Due to the large specific surface area of nanostructured materials, Fe_2O_3/metal oxide composites are prone to decomposition reactions between electrode materials and electrolytes, resulting in the formation of SEI films on the electrode surface, increasing irreversible capacity and reducing Coulombic efficiency [28]. Fe_2O_3 can effectively alleviate this problem by compounding with metal oxides, significantly improving the conductivity of electrode materials and the specific capacity of lithium-ion batteries.

CHAPTER 2. RESEARCH MATERIALS AND METHODS OF ENVISTIGATION

2.1. Peculiarities of the synthesis of transition metal nanooxides.

As you know, there are many methods of synthesis of nanooxides of transition metals and their nanocomposites, namely: pyrogenic, sol-gel, thermal decomposition method, chemical precipitation, solvothermal synthesis, synthesis in microemulsions of mechano-activation, etc. In this work, the following were used to obtain the original and mechanically activated nanocomposites: pyrogenic Al_2O_3; α-Fe_2O_3 was synthesized by the method of thermal decomposition.

2.1.1. Preparation of mechanically activated mixtures

Mechanical activation (from the English mechanical activation) – activation of bonds between surface atoms of particles of solid substances by mechanical processing. Grinding in a vibrating mill leads to the accumulation of structural defects, phase transformation and even amorphization of crystals, which affects the chemical activity of the mixture. As a result of high local pressures in some areas of the nanocomposite, tension is formed with subsequent relaxation.

Shock-vibration treatment (mechanical activation) of 80% Al_2O_3 + 20% α-Fe_2O_3 was performed in an Ardenne mechanical vibration mill. Mechanical activation took place in a metal reactor with a diameter of 25 mm using one metal ball with a diameter of 10 mm, at a frequency of oscillation of the reactor of 50 Hz. Preparation of all mechanoactivated samples in a vibrating mill was carried out for 5 minutes.

2.1.2. Preparation of starting mixtures.

The preparation of the starting mixture of 80% Al_2O_3 + 20% α-Fe_2O_3 was carried out by conventional mixing for 5 minutes in a mortar, followed by mixing in an Ardenne mechanical vibration mill for 3 seconds. The oscillation frequency of a metal reactor with a diameter of 25 mm using 1 ball of 10 mm was 50 Hz.

2.2. Methods of studying the electronic structure and features of their application to nano-sized oxides of transition metals

Currently, the study of the electronic structure of nanooxides of transition metals is a very promising area of research. There are many methods of theoretical calculation and correlation of calculations of electronic states of the valence band, however, modeling the atomic and electronic structure of nanoparticles is problematic because the shape, concentration, and distribution of defects in nanoparticles are unpredictable. Therefore, experimental methods of studying the energy distribution of valence electrons become very necessary. These include X-ray emission (RES) and photoelectron spectroscopy (PS). At the same time, RES enables the study of each of the bands of the studied sample separately, which allows to reject the influence of chemically non-interacting impurities that are part of this material on the distribution of valence electrons. This makes it possible to combine specific emission bands in a single energy scale and analyze the contribution of each of them to the complete picture of the distribution of electrons in the valence band. With the help of this method, it is possible to study both cast and powder, nanodisperse materials. Materials with high reactive properties with the environment, such as oxidation and carbonization, are investigated by these methods using surface treatment methods: mechanical cleaning, etching, annealing, argon-electron and electron beam bombardment. Therefore, the use of the RES method for the experimental study of the distribution of valence electrons comes first.

Ultrasoft X-ray emission spectroscopy. USXRES is one of the most informative methods for studying the distribution of electrons in the valence band [29, 30, 31]. This method reflects the energy distribution of valence electrons in the filled zone of certain symmetries, which are determined by X-ray series and selection rules. UMRE spectra reflect the energy distribution of valence electrons of surface and subsurface atoms located on one or two tens of atomic planes in the depth of the sample. Considering this and the fact that the study of nanometer-sized materials is a promising research area, the use of ultrasoft X-ray emission spectroscopy should be

considered an indispensable method for the study of nanomaterials.

The X-ray O*K*α-, Fe*L*α-, and Al*L*α- emission bands reflecting the energy distribution of the filled valence Or, Fe*sd*-, and Al*sd*-states, respectively, were obtained by the method of ultrasoft X-ray emission spectroscopy on the RSM-500 X-ray spectrometer-monochromator [31].

The anodic current in the study of the O*K*α-, Fe*L*α-, and Al*L*α-bands was chosen in such a way that it was sufficient to obtain contrast curves and, at the same time, so that the destruction of the sample was not observed. X-ray O*K*α-spectra were studied at the accelerating voltage in the X-ray tube U_a=5 kV and anode current I_a=5 mA, Si*L*α- and Al*L*α- bands at the accelerating voltage in the X-ray tube U_a=4 kv and anode current I_a=5 mA, and Fe*L*α- bands at the accelerating voltage in the X-ray tube U_a=7 kV and anode current Ia=7 mA, respectively. The spectra were obtained during oil-free vacuum pumping and additional freezing of hydrocarbon vapors with a nitrogen "trap" directly near the anode. The residual pressure in the X-ray tube and the volume of the spectrometer was 3.75×10^{-8} mm Hg. Art. To prevent thermal desorption of oxygen, as well as sintering of nanoparticles during measurements, test samples of a mixture of iron oxide and silicon dioxide were rubbed into the etched and washed with ethyl alcohol face of the copper anode, which was cooled with running water to a temperature of 10-15□.

In order to make sure that the O*Kα* band of the O*Kα* spectrum from CuO does not overlap with the O*Kα* band of the sample, the face adjacent to the sample was cleaned in the same way and the intensity of X-ray quanta was measured on it in the energy range hυ=510÷535 eV, which corresponds to the O*Kα* band of the mixtures. These measurements before and after the examination of the samples showed that the intensity of the quanta generated by the copper anode in the indicated energy interval did not exceed the level of the background intensity. To improve the reliability of the results, the data from the 4th-8th records of the emission bands were averaged.

X-ray radiation was decomposed into spectra by gold-coated diffraction gratings with a period of 600 mm−1 and a radius of curvature of 6 meters when measuring the O*Kα*- and Fe*Lα*- bands and with a filter mirror with a radius of

curvature of 4 m, and the AlLα band was obtained when using a grating and a mirror with radii curvature of 2 meters. The final filter mirror is coated with polystyrene to cut off wavelengths shorter than 4.4 nm. With slit widths of 10 μm, the hardware distortions measured by comparing the theoretical and measured widths of the Ti*Li*-line at ½ Imax in the region of wavelengths λ=31 Å did not exceed 0.2 eV, which in terms of wavelength λ=23.6 Å, where the O*Kα* band is located, is 0.3 eV. X-ray quanta were recorded using a secondary electron multiplier with a primary photocathode made of sputtered CsJ (KBL1500). The energy position of the O*Kα* and FeLα bands in the studied objects was determined relative to the CrLl line of the pure metal (in the second and first order of reflection, respectively). And the energy position of the Si*Lα*- and Al*Lα*- emission bands was determined relative to the ZrMξ line of the pure metal in the second order of reflection. The specified lines were used as benchmarks, the position of which was taken from tabular data.

The hardware distortion of the PCM-500 device when studying the above-mentioned transition metal nanooxides was ΔE≈0.2 eV and ΔE≈0.3 eV (when studying Al*L*α) (the hardware distortion was estimated by the energy broadening of the TiLi and ZrMξ lines of pure metals).

Processing of the received data was carried out in Microsoft Excel and OriginPro computer software. The analysis of the research results was carried out by comparing the received spectra normalized to one peak or background intensity.

2.3. Methods of studying the structure and morphology of nanooxides of transition metals

As previously mentioned, the number of atoms in mixtures, their structural arrangement, interaction between themselves and atoms of other chemical elements can lead to a change in the phase state, and therefore to a change in certain properties of nanooxides of transition metals. Therefore, there is a need to use the latest, highly precise, non-destructive methods of studying the morphology, chemical and phase composition of nanooxides.

2.3.1. Raster electron microscopy

Raster or scanning electron microscopy (SEM) has a number of advantages compared to other methods [32]. For example, compared to traditional light microscopy, it has a much higher resolution and depth of field; relative ease of interpretation of the obtained images due to their three-dimensional presentation; additional equipment can be connected for microscale analysiss. It is also necessary to note the relatively low requirements for the preparation of research samples. Compared to scanning probe microscopy, scanning electron microscopy allows you to examine significantly larger areas of the surface; work with highly embossed surfaces; use a much wider range of magnifications; to receive information not only about surfaces, but also about "subsurface" layers adjacent to the surface. One of the advantages of SEM is the possibility of determining the phase composition in certain areas of the sample [33].

The study of the surface and morphology, as well as the determination of the chemical composition of the mixtures, was carried out using a SEM-106Y scanning electron microscope (SELMI, Ukraine). Surface images of the research objects were obtained with high spatial resolution and depth of field in reflected (BSE) and secondary (SE) electrons. The resolution in the high vacuum mode is 4 nm. The limits of the permissible relative error of measuring the mass fraction of an element in the range from 12Mg to 92U in the composition of massive samples is no more than:

- ±4% for elements with a mass fraction range of more than 10%;
- ±20% for elements with a mass fraction range greater than 1% to 10%;
- ±50% for elements with a mass fraction range from 0.1% to 1%.

For a detailed study of the morphology and microstructure, photographs were taken at magnifications of x500 and x2500.

2.3.2. Transmission electron microscopy

A transmission (TEM) electron microscope is a device for obtaining an image of an ultrathin sample by passing a beam of electrons through it.

The method of transmission electron microscopy allows studying the internal structure of the materials under study, and in particular:

– Determine the type and parameters of the crystal lattice of the matrix and phases;

– Determine the orientational relations between the phase and the matrix;

– To study the structure of grain boundaries;

– Determine the crystallographic orientation of individual grains, subgrains;

– Determine the planar occurrence of defects in the crystal structure;

– To study the density and distribution of dislocations;

– To study the processes of structural and phase transformations in alloys;

– To study the influence of various technological factors on the structure of the material.

The disadvantage of the transmission electron microscope is that the samples need special preparation before direct studies, since it is necessary to make a sample of such a thickness that the electrons have a sufficient degree of passage through it.

Studies of the morphology and structure of the Al_2O_3+α-Fe_2O_3 mixture were carried out on a Philips CM30 transmission electron microscope at the Berlin Center for Materials and Energy. Helmholtz (Helmholtz-Zentrum Berlin fur Materialien und Energie, Hahn-Meitner-Platz 1, Berlin, Germany).

2.3.3. Peculiarities of using the X-ray phase analysis method to study the structure of oxides of transition metals.

Electron microscopy, along with obvious advantages (direct observation method), has a number of disadvantages, in particular, only a narrow zone of a specially prepared sample is analyzed. Therefore, among the entire range of methods of structural ordering and quantitative analysis, X-ray phase analysis occupies a prominent place. In this case, X-ray diffractometry becomes a powerful and

multifunctional tool for establishing the parameters of the microstructure of highly dispersed materials at the same time as determining their structural parameters.

X-ray research was carried out in monochromatic Cu K_α- radiation on a DRON - UM1 diffractometer. A graphite single crystal mounted on a diffracted beam was used as a monochromator. The diffractograms were obtained by the step scanning method in the range of angles 2θ 10-90°. The scanning step was 0.05°, the exposure time at the point was 3-7 s. Data processing of the diffractometric experiment was carried out using the Powder Cell 2.4 program for full-profile analysis of X-ray spectra from a mixture of polycrystalline phase components. The analysis of diffraction profiles and selection of the true physical broadening of the peaks was carried out by the method of approximations. The separation of the effects of the expansion of the diffraction maxima associated with the sizes of the coherent scattering regions and voltages of the II kind was carried out in the Hall-Williamson approximation. The crystallinity of the samples was determined by normalizing the integral intensity of the amorphous halo in the studied sample to the intensity of the corresponding amorphous halo in the completely amorphous sample. The studied powder nanocomposites were sprinkled into the cuvette without adding alcohol or other solvents, in order to avoid sedimentation of the nanocomposite.

2.4. Peculiarities of the electrochemical analysis method

The modern development of nanotechnology and nanoelectronics is closely related to portable sources of electric current. Improving the properties, namely the capacity and power of such sources is a very interesting direction for research. Therefore, the research direction of changing the distribution of valence electrons in the cathode materials of lithium power power (LPS) as a result of changing the particle size, changing the ratio of components or changing the synthesis method has a promising future.

The schematic diagram of LPS (Figure 2.1) includes [13]:

– Anode (metallic lithium or material containing lithium ions);

– Cathode (a material in which Li+ ions are intercalated into the channels of the crystal structure);

– Electrolyte (lithium-containing liquid, solid or gel-like material with an ionic type of conductivity).

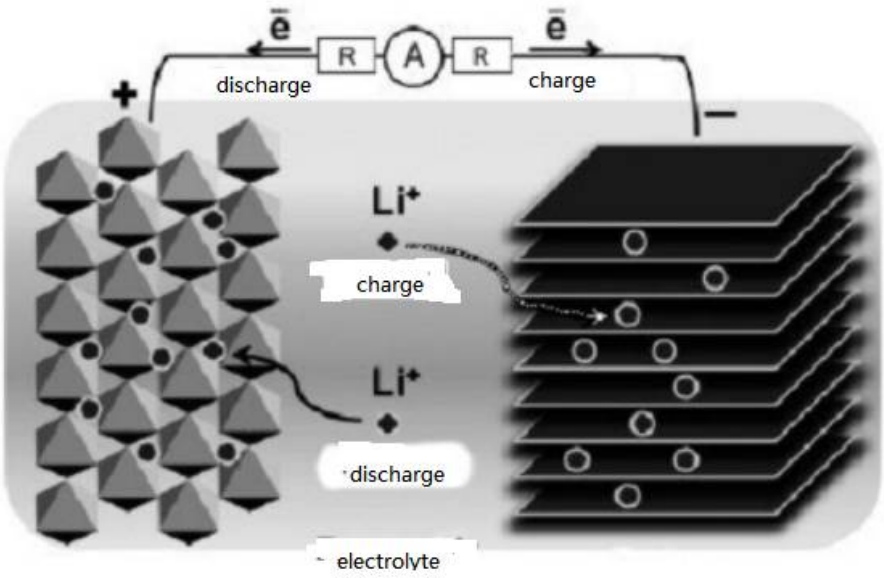

Figure. 2.1. Schematic diagram of LPS

When the circuit is closed, under the action of the potential difference between the anode and the cathode, the element discharges, lithium ions move from the anode to the cathode and are intercalated (introduced) into the structure of the latter. During the charging process, lithium ions are deintercalated (removed) from the cathode material (CM) and moved to the anode under the action of an electric field.

The study of charge capacities was carried out on a universal stand for studying the intercalation properties of TIONiT P2.00 LPS in the galvanostatic mode, all parameters at which cycling occurred were set on a computer connected to the device when using the MultiCycle software. The voltage range was chosen taking into account the chemical potentials of the cathode material and the anode material (metallic Li). When determining the optimal charge/discharge current, a current with a value of 0.1 of the theoretically calculated specific capacity of the LPS (0.1C) was selected. Results were processed using Microsoft Excel and OriginPRO programs.

When manufacturing LPS with the intercalation principle of action, in most cases it is necessary to increase the conductivity of the cathode composition by using conductive additives, which allows to achieve higher values of the discharge current [34].

Research of LPS layouts under the conditions of traditional operating currents consumed by such systems requires the use of electrochemical cells with a larger contact area at the electrode-electrolyte boundaries and a shorter distance between the electrodes. This ensures high exchange current values and significantly reduces electrolyte consumption.

A round lithium foil of the appropriate diameter served as the anode. The separator was non-woven propylene of a slightly larger diameter. The cathode was formed as follows: a mixture of cathode-active material (the studied samples), a conductive additive (carbon black) and a binding agent (PVA dissolved in n-methyl) was applied to a separator paper that had the same shape and dimensions as the lithium anode. After that, the obtained electrodes were dried at a temperature of 100°C for 2 hours. As a result, electrochemical cells were formed using a non-aqueous electrolyte - $LiPF_6$ with a solvent - butyrolactone.

The results of the operation of the electrochemical cell in the galvanostatic mode are presented with the help of graphs, where the specific capacity is laid down on the abscissa axis, and the voltage recorded by the device is on the ordinate axis. The specific capacity is calculated by the formula.

$$C_n = \frac{It}{m} \tag{2.1}$$

I– constant current, which we set independently, is the time during which the cell is charged (discharged), is the mass of the cathode substance. The specific capacity is one of the extremely important characteristics of an electrochemical cell, which is directly related to the ability of the structure of the cathode material to accumulate lithium ions.

When using a cathode material (SUM) based on initial and mechanoactivatedmixtures, the current generation process can be written as

$$xLi^{+} + xe^{-} + SUM \rightarrow Li_x\ SUM\ , \qquad (2.2)$$

x – the value of the "guest" load or the degree of intercalation, in other words, x is the number of introduced lithium ions per one formula unit of the "host" material, which was determined from the ratio

$$x = (nF)^{-1} \frac{M}{m} q \qquad (2.3)$$

or

$$x = (nF)^{-1} \frac{M}{m} It \qquad (2.4)$$

n – the number of electrons participating in the reaction from the hydroxide-reduction process, F is the Faraday constant, M and m are the molar mass and mass of the sample of the “host” material, respectively, q is the amount of passed electricity, I is the discharge current, t is the discharge time.

CHAPTER 3. THE RESULTS OF THE EXPERIMENT

The literature review describes the occurrence of interatomic interaction as a result of mechanoactivation in mixtures of aerosols and oxides of transition metals. These studies revealed that the nature of the specified interatomic interaction depends significantly on both the chemical composition of the components and the type of their crystal structure. Since the components of previous studies were amorphous SiO_2 and crystalline nanooxides, there is an interest in studying the influence of mechanoactivation on the nature of the interaction in mixtures where the components are crystalline modifications of nanooxides. Taking into account the fact that in the work [35] an interatomic interaction was found between aerosol and nanosized Al_2O_3 oxide, with smaller differences in the energies of the valence band ceilings of SiO_2 and Al_2O_3 than in the cases of pure SiO_2 and α-Fe_2O_3, it is worth studying the effect of mechanoactivation treatment on the structure and interatomic interaction in Al_2O_3+α-Fe_2O_3 mixtures depending on the ratio of components. To do this, consider a comparison of the energy distributions of valence electrons in Al_2O_3 and α-Fe_2O_3 by combining in a single energy scale AlLα- (alsd-electron distribution), OKα- (Op-electron distribution) and FeLα- (Fesd-electron distribution) spectra (Figure.3.1).

From this combination (Figure 3.1), it can be seen that the difference in the energies of valence band ceilings in the initial Al_2O_3 and α-Fe_2O_3 is slightly smaller than that observed for SiO_2 and α-Fe_2O_3 and larger than that observed for SiO_2 and Al_2O_3. The decrease of this difference for Al_2O_3 and α-Fe_2O_3 compared to SiO_2 and α-Fe_2O_3 indicates a decrease in the potential barrier of interaction between Al_2O_3 and α-Fe_2O_3 compared to the barrier of SiO_2 and α-Fe_2O_3. Therefore, to study the impact of shock-vibration treatment on interatomic interaction, it is necessary to study the energy and charge distribution of valence electrons depending on the composition of the mixtures.

The energy difference in the ceilings of the valence bands of Al_2O_3+ α-$Fe_2O_3$3 can contribute to the processes of intercalation of Li^+ ions in the crystal structure of the channels of the LPS cathode material. Therefore, in this section, the impact of

shock-vibration treatment of Al_2O_3+ α-Fe_2O_3 mixtures on the charge capacity of LPS with cathodes based on them should be studied.

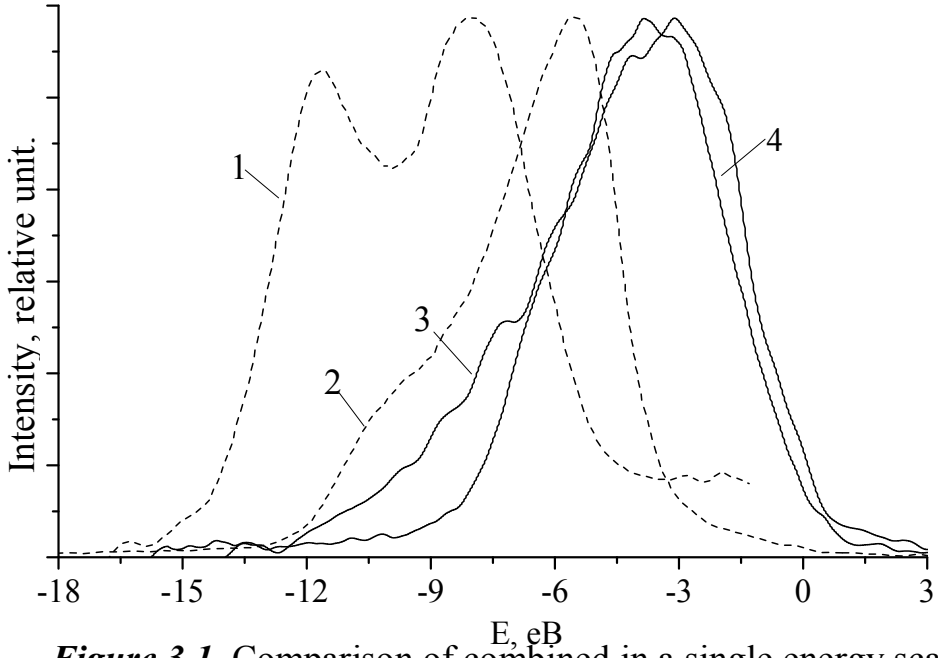

Figure 3.1. Comparison of combined in a single energy scale 1-AlLα and 2-OKα spectrum from the original Al_2O_3 and 3-FeLα and 4-OKα spectrum from the original α-Fe_2O_3.

3.1. Change in morphology of mixtures after mechanical activation

In order to understand how mechanical activation affects the distribution of electrons in the valence band, it is necessary to consider the impact of shock-vibration treatment on the morphology of the initial precursors and the mixture with a ratio of 80 wt. % Al_2O_3 and 20; mass % α-Fe_2O_3. In Figure.3.2 shows the morphology of α-Fe_2O_3 before and after treatment [36]. As can be seen from this image, slight grinding of crystallites occurs during mechanoactivation. Therefore, we will consider the effect of this method on the morphology of the initial Al_2O_3 (Figure.3.3). It can be seen from this Figure that the mechanical activation of aluminum oxide leads to the grinding of agglomerates consisting of nano-sized particles, namely, in a simple mixture, the size of agglomerates was 10-130 μm, while after mechanical activation, the size of agglomerates decreased to 1-30 μm. In addition, it is clearly visible that the morphology of the mechanically activated Al_2O_3 powder is much denser.

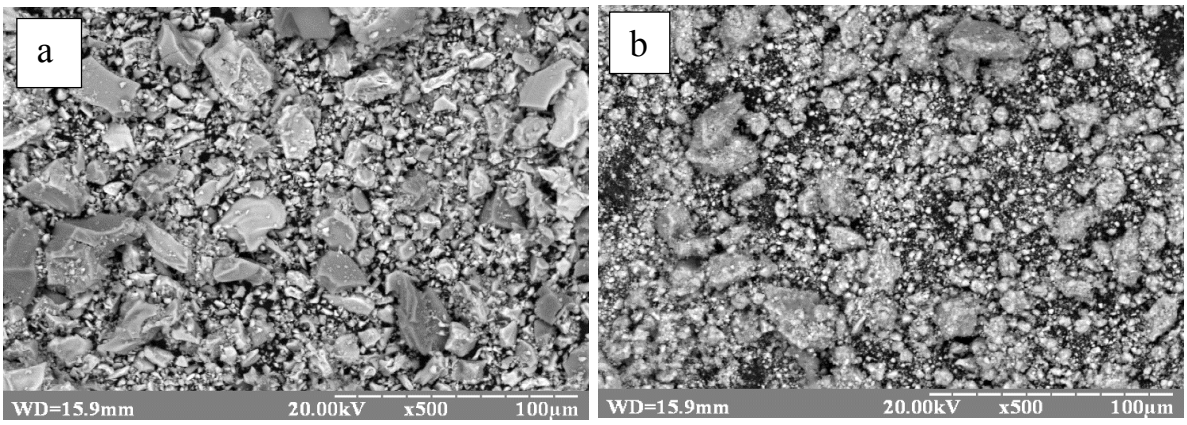

Figure 3.2. SEM image of α-Fe_2O_3 before (a) and after (b) mechanical activation, x500 [36].

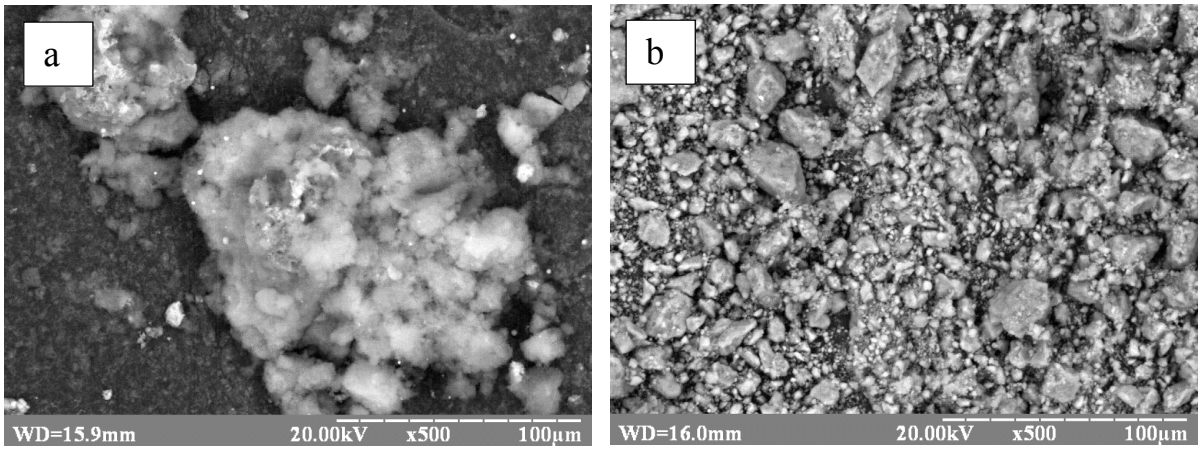

Figure 3.3. SEM image of Al_2O_3 before (a) and after (b) mechanical activation [36].

Since the chemical potentials of Al_2O_3 and α-Fe_2O_3 differ, we will consider how mechanical activation affects the morphology of mixtures with different mass ratios of components. The analysis of the point chemical composition data (Figure 3.4) of $0.8Al_2O_3$+0.2α-Fe_2O_3 before and after mechanoactivation showed that in the initial mixtures, the lighter grains correspond to α-Fe_2O_3, and the darker ones correspond to translucent Al_2O_3 (Table.3.1.). At the same time, iron and aluminum are simultaneously present in mechanoactivated particles, although their ratio differs at different points. This indicates that after mechanoactivation the formed grains consist of iron and aluminum oxides.

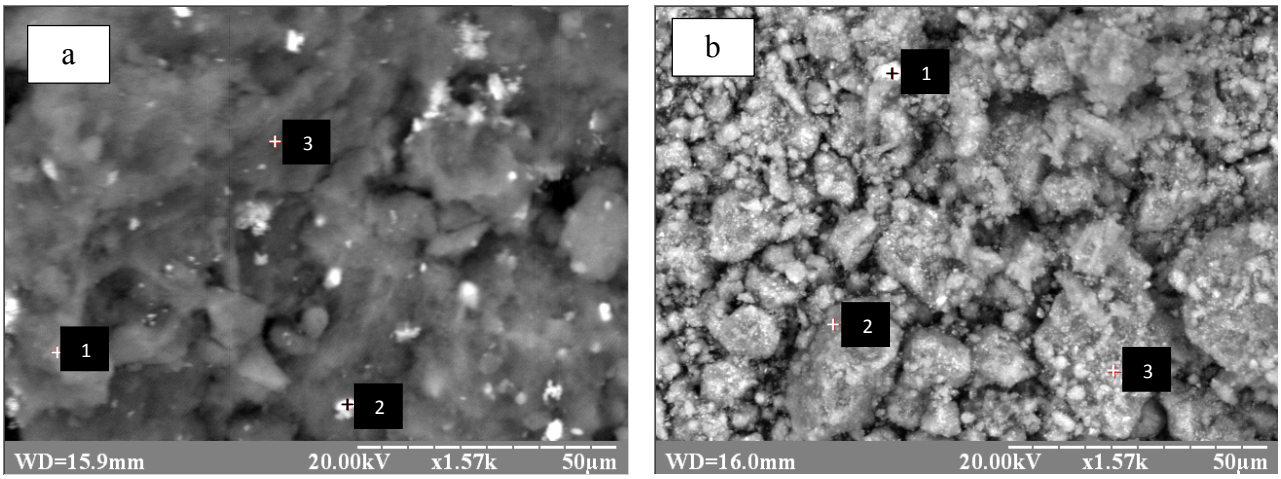

Figure 3.4. SEM image of nanocomposite 80% Al_2O_3+20% α-Fe_2O_3 before (a) and after (b) mechanical activation x1500.

Table .3.1. Point chemical composition of mixtures 80% Al_2O_3+20% α-Fe_2O_3 before and after mechanical activation

Mixture	Point	Fe, %	Al, %
80% Al_2O_3+20% α-Fe_2O_3	1	3,7	96,3
	2	98,8	1,2
	3	30,5	69,5
80% Al_2O_3+20% α-Fe_2O_3 (treated)	1	86,8	13,2
	2	25,8	74,2
	3	44,2	55,8

Now we will consider in more detail the influence of mechanovetivation on the morphology of the mixture. As can be seen from (Figure.3.5a, Figure.3.6a), oxide nanoparticles of the original mixture are evenly distributed throughout the volume of the mixture without the formation of any specific structure.

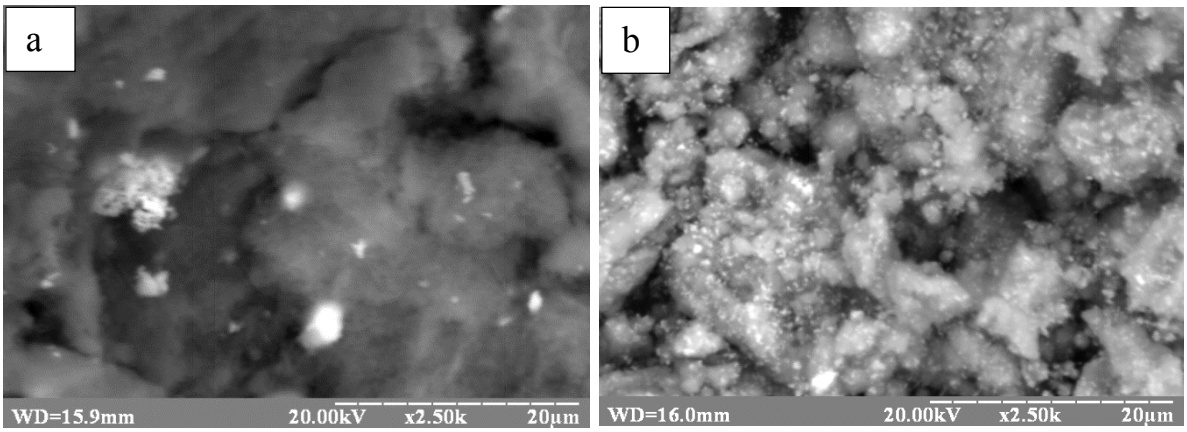

Figure 3.5. SEM image of nanocomposite 80% Al_2O_3+20% α-Fe_2O_3 before (a) and after (b) mechanical activation x2500

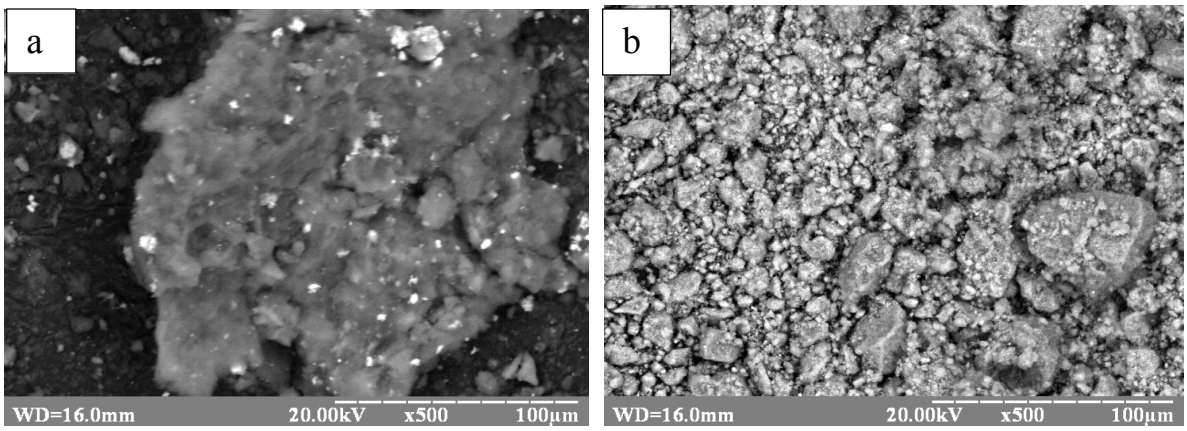

Figure 3.6. SEM image of nanocomposite 80% Al_2O_3+20% α-Fe_2O_3 before (a) and after (b) mechanical activation x2500.

At the same time, the formation of agglomerates with a pronounced structure (Figure.3.5b, Figure.3.6b) with sizes of 1-5 and 20-60 microns is observed in mechanically activated mixtures. At the same time, α-Fe_2O_3 agglomerates from 2-10 μm to sizes smaller than 1 μm are broken down, and these particles are evenly distributed throughout the volume of the nanopowder mixture (Figure.3.5b). Since mechanical activation causes agglomeration of the original Al_2O_3, the crushed α-Fe_2O_3 nanoparticles due to the specified treatment are obviously mechanically embedded in aluminum oxide agglomerates.

When examining the TEM images of the initial mixture of 80% Al_2O_3+20% α-Fe_2O_3 (Figure 3.7), it can be seen that the particles have an ordered, crystalline structure, while no interaction between nanoparticles is observed. At the same time, in the mechanoactivated mixture, smaller Al_2O_3 nanoparticles are embedded into larger α-Fe_2O_3 particles.

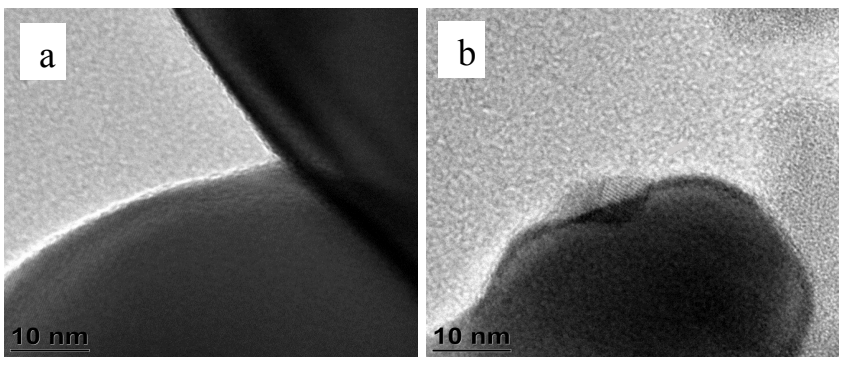

Figure 3.7. TEM image of 80% Al_2O_3+20% α-Fe_2O_3 before (a) and after (b) mechanical activation.

3.2. Studying the structure of the composite using X-ray diffraction

Let's analyze how the shock-vibration treatment method affects the structure of the studied mixture of 80% Al_2O_3+20% α-Fe_2O_3, considering the impact of shock-vibration treatment on the structural characteristics of the original Al_2O_3 and α-Fe_2O_3 [36]. When analyzing the X-ray pattern of the initial and mechanoactivated α-Fe_2O_3 (Figure 3.8a), it was found that the phase composition of both samples consists of 100% of the alpha phase of Fe_2O_3 (Table 3.2). At the same time, the area of coherent scattering in the mechanoactivated sample of the original α-Fe_2O_3 decreases by 2 nm, which is within the experimental error. At the same time, changes in the lattice parameters due to the mechanoactivation of α-Fe_2O_3 are within the experimental error (Table 3. 3).

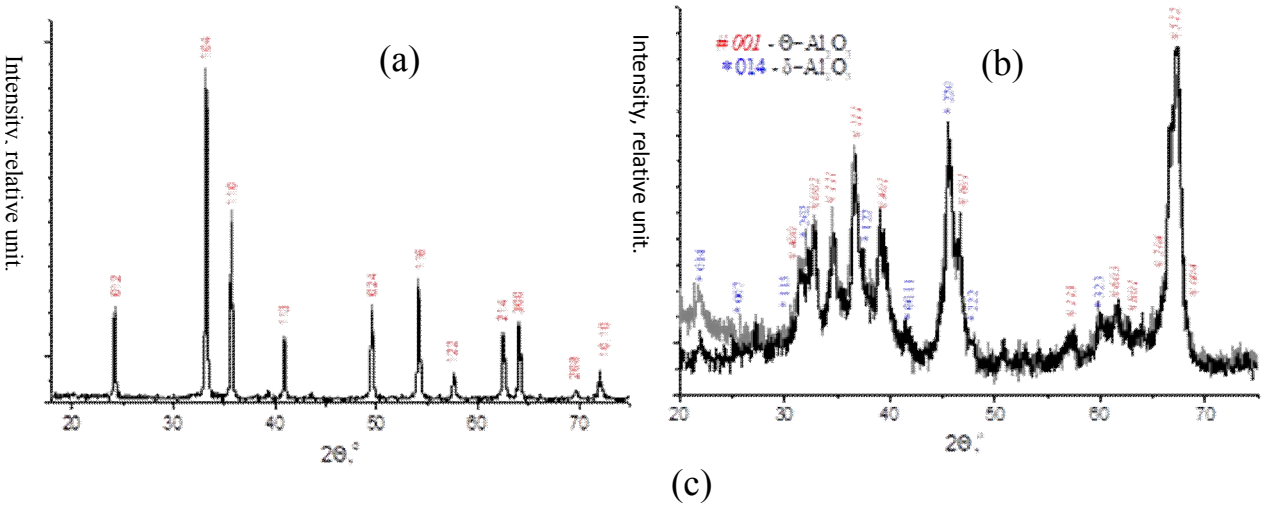

Figure 3.8. X-ray pattern of the initial and mechanoactivated α-Fe_2O_3(a), Al_2O_3 (b) [36]

When analyzing the X-ray diffractogram from the original Al_2O_3 (Figure 3.8b) [36], it was found that the phase composition of the original mixture consists of 78.8% theta phase and 21.2% delta phase Al_2O_3. At the same time, in the mechanically activated sample, the content of the Θ and δ phases of aluminum oxide is 82.9% and 17.1%, respectively, which indicates a decrease in the content of the δ phase by 4.1% and an increase in the Θ phase of aluminum oxide by the same amount

(Table 3.2). In addition, as a result of mechanical activation, the OCR Θ and δ of the Al_2O_3 phase increases by 10 and 12 nm. At the same time, the changes in lattice parameters due to the mechanical activation of Al_2O_3 are within the experimental error (Table 3.3) [36].

Table 3.2. Phase composition, sizes of OCR (D) and change of OCR (ΔD) in the α-Fe_2O_3 and Al_2O_3 due to treatment [36].

Sample	Phase composition, mass %	D, nm	Δ D, nm
α-Fe_2O_3	α -Fe_2O_3 - 100	α - 92	α -2
α -Fe_2O_3 (treated)	α -Fe_2O_3 - 100	α - 90	
Al_2O_3	θ-Al_2O_3 – 78.8	θ - 35	θ +10 δ +12
	δ-Al_2O_3 – 21.2	δ - 47	
Al_2O_3 (treated)	θ-Al_2O_3 – 82.9	θ - 45	
	δ-Al_2O_3 – 17.1	δ - 59	
Error	±5%	±3-8*нм*	±3-8*нм*

Table.3.3. Lattice parameters (a, b, c, β) of initial and mechanically activated initial components; Δ is a change in the lattice parameter [36].

		Gratti parameters, nm							
		α-Fe_2O_3, *нм*		δ-Al_2O_3, *нм*		Θ-Al_2O_3, *нм*			
		a	*c*	*a*	*c*	*a*	*b*	*c*	*β,°*
Fe_2O_3	1	0.5033	1.3745	-	-	-	-	-	-
	2	0.5035	1.3750	-	-	-	-	-	-
	Δ	***0.0002***	***0.0005***	**-**	**-**	**-**	**-**	**-**	**-**
Al_2O_3	1	-	-	0.5634	2.3482	1.1839	0.2925	0.5626	103.79
	2	-	-	0.5632	2.3473	1.1835	0.2921	0.5620	103.60
	Δ	**-**	**-**	***-0.0002***	***-0.0009***	***-0.0004***	***-0.0004***	***-0.0006***	***-0.19***
Error		0.0005-0.001 *нм*							$0,7^o$

Comparing the results of X-ray phase analysis (Table 3.4) of the original and mechanoactivated mixture of 80% Al_2O_3+20% α-Fe_2O_3 (Figure.3.9) shows that the phase composition of the mixtures corresponds to the mass ratio of the components with minor deviations. At the same time, mechanical activation is accompanied by an

increase in the size of α-Fe_2O_3 and Al_2O_3 crystallites by 11-12 nm. However, no changes in lattice parameters are observed (Table 3.5). Such an increase in OCR is possibly to consequence of layering of crystallites on top of each other.

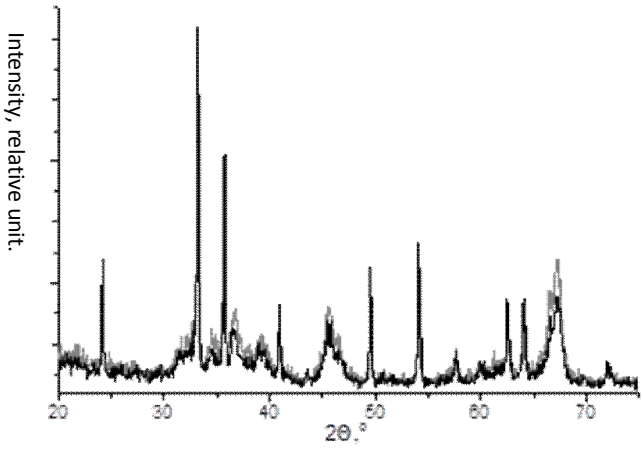

Figure 3.9. X-ray pattern of the initial and mechanoactivated α-Fe_2O_3(a), Al_2O_3 (b), 80% Al_2O_3+20% α-Fe_2O_3(c)

Table 3.4. Phase composition, sizes of OCR (D) and change of OCR (ΔD) in the samples 80% Al_2O_3+20% α-Fe_2O_3 due to treatment

Sample	Phase composition, mass %	D, nm	Δ D, nm
80% Al_2O_3+20% α-Fe_2O_3	α-Fe_2O_3 – 17.4	α - 86	α +13 θ +11 δ +11
	θ-Al_2O_3 – 65.1	θ - 30	
	δ-Al_2O_3 – 17.5	δ - 42	
80% Al_2O_3+20% α-Fe_2O_3 (treated)	α-Fe_2O_3 – 19.6	α - 99	
	θ-Al_2O_3 – 61.5	θ - 41	
	δ-Al_2O_3 – 18.9	δ - 53	
Error	±5%	±3-8*нм*	±3-8*нм*

Table 3.5. Lattice parameters (a, b, c, β) of initial and mechanically activated mixtures of 80% Al_2O_3+20% α-Fe_2O_3; Δ is a change in the lattice parameter.

		Gratti parameters, nm							
		α-Fe_2O_3, *нм*		δ-Al_2O_3, *нм*		Θ-Al_2O_3, *нм*			
		a	*c*	*a*	*c*	*a*	*b*	*c*	*β,°*
80% Al_2O_3 + 20% Fe_2O_3	1	0.5036	1.3758	0.5630	2.3483	1.1836	0.2922	0.5624	103.47
	2	0.5035	1.3752	0.5625	2.3473	1.1827	0.2919	0.5634	102.93
	Δ	***-0.0001***	***-0.0006***	***-0.0005***	***-0.0010***	***-0.0008***	***-0.0003***	***0.0010***	***-0.54***
Error		0.0005-0.001 *нм*							0,7°

3.3. Features of valence electron distribution in a mixture of 80% Al_2O_3+20% α-Fe_2O_3 before and after mechanical activation

When studying the energy redistribution of valence electrons in the OKα and AlLα spectra of crystalline Al_2O_3, the energy distribution of the Or and Alsd electronic states was identified based on a comparison of the AlLα and OKα bands with data from theoretical calculations of the densities of the Alsd and Or electronic states [35] , where it was shown that the subbands in the low-energy region of the OKα and AlLα spectra [37] reflect covalently binding Als+O2p states, while the high-energy peaks of the OKα bands reflect non-binding states populated by transferred from Al atoms electrons At the same time, the second maximum of the AlLα band in the high-energy region obviously reflects Alsd electrons not involved in the bond, since the presence of Als electrons in this energy region is negligible. As it was shown [38], in the region of the minimum of the AlLα band and in the region of energies corresponding to the low-energy contour of OKα, three clear subbands are observed, which obviously reflect Or π states, which was indicated in the calculations of the linear combination of atomic orbitals of Al_2O_3 [39].

The energy ranges in which the Op- and Fesd-valence electrons are concentrated were determined in Chapter 5 of the dissertation by combining the OKα and FeLα spectra in a single energy scale, as well as theoretical calculations of the partial densities of states. From this comparison, it can be seen that the OKα band mainly reflects the O2p states of oxygen strongly hybridized with Fe3d orbitals, while the weak features of the OKα band are in the same energy ranges as in the Van Hove features in the Op- and Fe3d densities - became From the comparison, in the same section, of the FeLα and OKα bands, it can be seen that their shape is quite similar with the exception of the low-energy region, where the "a" band in the FeLα band, which reflects the high density of Fe3d states, is three times larger than the density of Op states and is separated from the high-energy region by a deep minimum. Since the shape of the curves reflecting the densities of Op states and Fe3d states are extremely similar, these states are highly hybridized. Despite the fact that

the contribution of Fe3d states in the high-energy region is two times smaller, this indicates a high degree of covalency of Fe-O bonds.

Comparison of the Okα and AlLα-bands before and after Al_2O_3 mechanoactivation (Figure 3.10) did not reveal any differences in the shape and energy position of the OKα band, and minor deviations are within the experimental error.

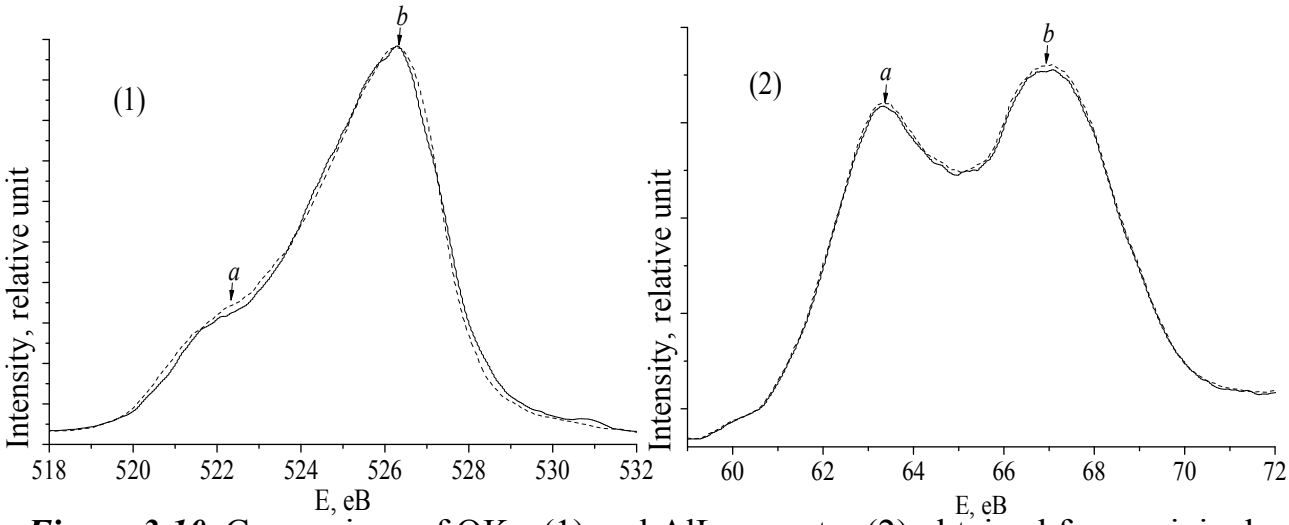

Figure 3.10. Comparison of OKα-(1) and AlLα-spectra (2) obtained from original and mechanically activated Al_2O_3. Dashed line – initial Al_2O_3, solid line – mechanically activated Al_2O_3.

When comparing the OKα and FeLα bands before and after the mechanoactivation of α-Fe_2O_3 (Figure 3. 11), no significant differences were found in the shape and position of the bands, with the exception of a slight narrowing, which is obviously a consequence of the partial dehybridization of the Fed+Op states when the

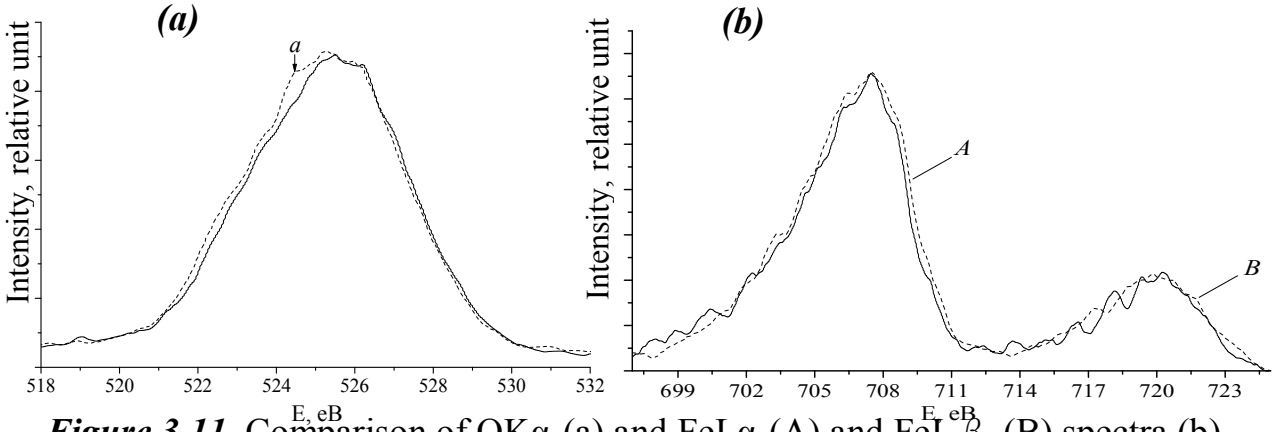

Figure 3.11. Comparison of OKα-(a) and FeLα-(A) and Fe$L\beta$ -(B) spectra (b) obtained from the original and mechanically activated Al_2O_3. Dashed line – initial Al_2O_3, solid line – mechanoactivated α-Fe_2O_3.

ion- of covalent bonds during grinding of nanoparticles [36].

Consider a comparison of the OKα bands of the mixture of 80% Al_2O_3+20% α-Fe_2O_3 (Figure.3.12) [40]. From this comparison, it can be seen that the mechanoactivation of the mixture is accompanied by a narrowing of the spectrum in the range of energies (526÷528) eV of the OKα band in the low-energy side by 0.1-0.3 eV. Such a narrowing of the OKα bands indicates a decrease in the occupancy energies of Op electrons in this region as a result of transfer to other ions or due to a decrease in the energy of Op states.

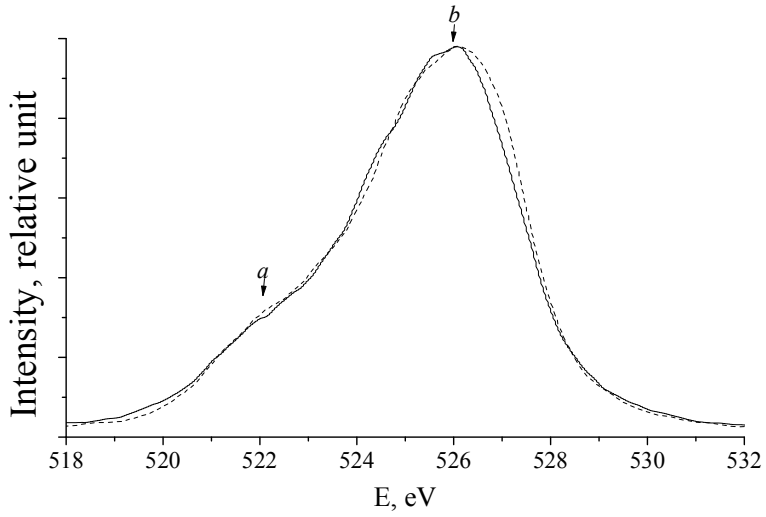

Figure 3.12. Shift of contours of OKα bands as a result of mechanical activation of a mixture of 80% Al_2O_3+20% α-Fe_2O_3. The dashed line is the OKα band of the mixture, the black line is the OKα band of the mechanoactivated mixture.

Therefore, we will consider the comparison of AlLα bands before and after mechanoactivation (Figure.3.13). From this comparison, it can be seen that the high-energy contour of the AlLα-band in the mechanoactivated mixtures is shifted to the long-wavelength side by 0.2-0.3 eV relative to such a contour in the original mixture. At the same time, the intensity of the high-energy peak of the AlLα band decreases. This also indicates a decrease in the population of Alsd-hybrid states. Such a decrease in Op- and Alsd- electronic states is most likely a consequence of the breaking of

bonds due to the injection of smaller and harder Al_2O_3 nanoparticles [41] into larger α-Fe_2O_3 nanoparticles under high local pressures during shock-vibration processing.

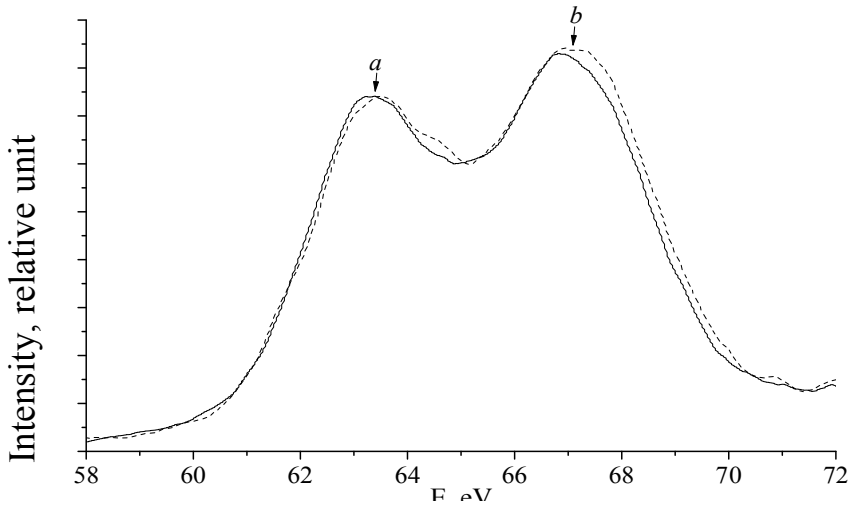

Figure 3.13. Comparison of the contours of AlLα - bands of a mixture of 80% Al_2O_3+20% α-Fe_2O_3, hatched line - AlLα - a band of the mixture, black AlLα - a band of mechanoactivatedсуміші.

3.4. The influence of mechanical activation on the charge capacity of lithium energy sources

Since changes in morphology, structure and minor changes in the electronic structure occur as a result of shock-vibration treatment of 80% Al_2O_3+20% α-Fe_2O, we will consider the effect of this method on the charge capacities of LPS with cathodes based on a mixture of 80% Al_2O_3+20% α-Fe_2O_3 (Figure 3.13).

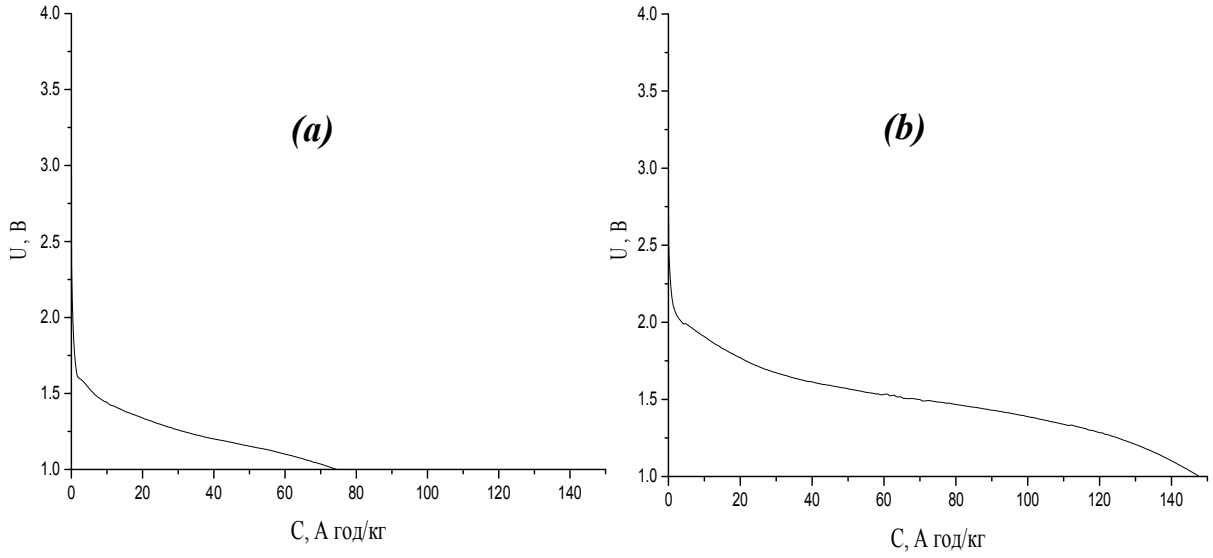

Figure 3.14. Discharge curves of the 80% Al_2O_3+20% α-Fe_2O_3 mixture before (a) and after (b) mechanical treatment

It can be seen from (Figure 3.13a) that the charging capacity of the LPS with a cathode based on the original mixture is 72 A·h/kg. On the other hand, the charge capacity of LPS with cathodes based on the mixture after mechanical activation is 148 A·h/kg. That is, it can be stated that the charging capacity of the LPS with a cathode based on a mechano-activated mixture has doubled (Figure 3.13b). Such an increase in the charge capacity is most likely a consequence of the injection of Al_2O_3 nanoparticles into α-Fe_2O_3 and an increase in the surface defects of the nanoparticles of the mechanically activated mixture. After all, from the results of SEM and TEM, an increase in the number and density of agglomerates was established, from X-ray diffraction, an increase in the size of the region of coherent expansion was established, and from UMRES, a slight decrease in the population of electrons in the high-energy region of p-states of oxygen and s, d-states of aluminum was established.

CHAPTER 4. OCCUPATIONAL HEALTH AND SAFETY IN EMERGENCIES

4.1 General provisions

Labor protection includes the legislative system, socio-economic, technical, health, and treatment and preventive measures to ensure the safety, health and efficiency of workers.

Safety and industrial hygiene is a system of organizational measures and technical means to prevent dangerous and harmful production factors from affecting employees. Risk factors include causing workers to be injured or their health conditions suddenly and drastically deteriorated. On the contrary, harmful production factors can cause workers to get sick or reduce efficiency.

Therefore, the first condition for completing the master's thesis is to ensure the job security of the research engineer. Eliminate the possibility of scientific laboratory

equipment causing harm to workers, create normal working conditions, and eliminate the influence of harmful factors that cause occupational diseases. Proper calculation and measures to eliminate the influence of harmful factors on the human body are one of the main contents that must be formulated at the beginning of the master's thesis, because the health and efficiency of the staff depend on it.

4.2 Analysis of Harmful and Dangerous Production Factors（HDPF）

The paper investigates the effect of mechanical processing on the structural characteristics of the initial components of nanosized Al_2O_3 and Fe_2O_3 powders and a mixture of 80% Al_2O_3/20% Fe_2O_3. The relationship between the change in structural characteristics and the capacities of lithium current sources with electrodes based on mixtures before and after treatment was established.

During the experiment, Ardenne mechanical vibration mill, X-ray diffractometer, SEM scanning electron microscope, lithium power supply and other equipment were used. Mechanical vibration may cause mechanical damage to people and generate noise, nano-level powder will cause dust pollution, X-ray and other analytical instruments will produce radiation, and all electrical equipment will have electrical safety hazards, etc. This chapter will analyze the unsafe factors existing in the experiment process and propose solutions.

4.2.1 Working space

The dimensions of the lab grounds and windows were measured:

- dimensions of the laboratory : width (6 m), length (8 m), height (3.2 m);
- Window size : width (2 m), height (1.8 m).

We will calculate the area and volume:

The laboratory area is:

$$S=a\times b=6\times 8=48\ m^2$$

The laboratory volume is:

$$V=a\times b\times c=6\times 8\times 3.2=131.6\ m^3$$

According to ДБН В.2.2-28-2010 [42], the area norm per person is 4.5 m^2, and the room volume norm per person is 16 m^3.

Let's calculate the area and volume per person for this audience, provided that the number of employees is three:

$$S_p=48/3=16\ m^2;$$

$$V_p=154.6/3=51.2\ m^3.$$

So the laboratory space meets the standards.

4.2.2 Microclimate in the laboratory work area

It is very important for the laboratory environment to have the best temperature, humidity and clean air at a certain flow rate for the normal life and work performance of the human body, so the microclimate of the laboratory work area is studied. The main components are: temperature, humidity, and air mobility. According to ДСН 3.3.6.042-99 [43] "Hygienic specifications for the microclimate of industrial plants", the division of cold and warm periods is distinguished according to the seasons.

The research results of microclimate parameters in the laboratory working area are shown in Table 4.1.

Table 4.1. Values of microclimate parameters for laboratory working areas.

Period	Air temperature, □		Air humidity, %		Air speed, m/s	
	Measured	Acceptable	Measured	Acceptable	Measured	Acceptable
Cold	18	21~24	65	<75	0.18	<0,2
Warm	26	21~28	45	<55	0.24	0.1~0.3

The results of the microclimate study show that according to the standard established by ДСН 3.3.6.042-99 [43], the microclimate does not fully meet the allowable standard and has adverse effects. The microclimate indicators in the warm

season throughout the year are within an acceptable range. Although there is heating supply in winter, due to the large laboratory area, it cannot meet the overall temperature requirements.

4.2.3 Light Analysis

Lighting is generally divided into three types: natural lighting, artificial lighting and combined lighting. The laboratory uses a combination lighting system: a lighting system that uses natural and artificial lighting during the dark hours of the day. In visual working conditions, natural lighting alone is not sufficient and is supplemented by artificial lighting in accordance with ДБН В2.5-28-2006 [44].

The natural lighting of the laboratory is provided through the windows. During daylight hours, daylighting fully complies with established standards, saving electricity. Artificial lighting fixtures are evenly placed in the upper area of the room. When lighting does not meet established specifications, workers can experience impaired vision, headaches, and difficulty concentrating over long periods of time, leading to inaccurate job performance.

4.2.4 Noise analysis

The operation of laboratory equipment (especially fans, burners, grinders, etc.) is accompanied by noise, vibration or ultrasound. The continuous impact of these factors has adverse effects on human health. Noise can cause premature fatigue and have adverse effects on the nervous system, increasing the likelihood of injury. Excessive vibrations lead to persistent impairment of the body's physiological functions: circulatory disturbances under the influence of vasospasm, loss of skin sensitivity, reduced joint mobility. Noise, vibration and ultrasound are the result of mechanical vibrations that propagate from the source of the vibration through the environment. The human ear perceives vibrations as sound if the frequency is in the range of 16 to 20,000 Hz. Fluctuations in frequency from Hz particles to 12 Hz are perceived by humans as individual shocks. The high-frequency oscillations directly perceived by the human body are related to vibration. Vibratory oscillations with a

frequency of 6-9 Hz, which can be directly perceived by humans, are a serious danger, since the largest internal organs have their own oscillation frequencies within the same limits, and dangerously disturbing resonances of function can occur in the beginning. Under production conditions, noise is perceived by the human ear as sounds passing through the air in varying intensities and tones. ССБТ (ДСН 3.3.6.037-99) [45] specifies the permissible noise levels and general requirements for noise protection in workplaces.

When working in environments with high noise levels, earplugs should be worn to avoid injury.

4.2.5 Radiation

There is a risk of ray radiation during the operation of X-ray diffractometers and SEM scanning electron microscopes. However, strict maintenance inspection requirements and operating guidelines for such instruments in the future, and users can operate under the guidance of teachers and instruction books to avoid ray radiation damage.

4.3 Engineering solutions

4.3.1 Electrical Safety

All laboratory equipment is powered by a 380 V power supply. The equipment used is a Class I and Class II electrical product according to ПУЕ-2017 [46] Methods of Protection of Persons from Electric Shock.

Construction requirements for electrical installations are given in the Regulations for Arrangement of Electrical Installations (ПУЕ-2017) [46] for electrical installations under construction or renovation with a voltage not exceeding 500 kV. According to the PNE, premises are classified into three categories according to the risk of electric shock injury, depending on whether there is an element of increased or special risk of electric shock injury in the space. Following this investigation, there are no particularly dangerous elements present in the laboratory.

During the use of electrical equipment, there may be a risk of electric shock. Mainly due to easy access to current-carrying parts of the equipment due to damaged wire insulation; voltage on de-energized current-carrying parts due to incorrect connection of the device; unsatisfactory or incorrect operation of the equipment, operator inattention, etc. Reason [47].

To ensure the electrical safety of workers, the following measures are adopted: regular inspection of insulation status, inaccessibility of live parts, and timely training and knowledge testing of operators on electrical safety issues, distribute insulating gloves and safety shoes.

4.3.2 Ventilation of laboratory premises

The air extractor is selected according to the experimental process and the type of equipment, it must ensure the necessary cleanliness of the air in the workplace and minimize the consumption of removed air, prevent the spread of harmful substances in the room and not interfere with technical operations. Suctioning of the equipment is imperative in order to be as close as possible to sources of harmful emissions. Typical schemes and designs of suction pumps and their calculation methods are summarized in the Design Guide [48].

The volume of air to be exhausted or supplied by the ventilation system (air exchange volume L required for the production site in m^3/h) is determined by different methods depending on the specific conditions: from empirical formulas or recommended air exchange volumes.

In general, the intensity data of harmful substances released into the atmosphere by indoor air exchange is calculated by the following formula:

$$L = \frac{1000\beta V}{C_{ex} - C_{in}} \quad (4.1)$$

where V is the intensity of the release of harmful substances per unit time g/h; β - coefficient of uneven distribution of harmful substances in the volume of the room; C_{ex}, C_{in} - concentration of harmful substances in the air exhaust and incoming (inflow), mg/m^3.

For general exchange ventilation β it is recommended to take from 1.2 to 2.0: smaller values - for low-toxic substances and with a relatively uniform distribution of sources of their formation; maximum - for more toxic substances with their uneven release.

Concentrations of harmful substances in the exhaust and supply air Cex, Cin are taken as follows. The concentration of harmful substances in the supply air should be minimal and not exceed 30% of the MAC in the air of the working area, and in the exhaust air should not exceed the MAC in the air of the working area [49]. Therefore, the value of Cex is usually taken to be equal to the maximum concentration limit. Then the general formula 1.1 takes a more specific form:

$$L = \frac{1000\beta V}{C_{MAC} - C_{in}} \quad (4.2)$$

If the air is removed from the work area and $C_{in} = 0$

$$L = \frac{1000\beta V}{C_{MAC}} \quad (4.3)$$

If from the upper zone, then

$$L = \frac{1000\beta V}{K_a C_{MAC}} \quad (4.4)$$

Where K_a - air exchange coefficient (has a value of 0.9 ~ 1.1 when supplying air with horizontal jets; 1.65 ~ 1.85 - when supplying to the working area; 1.25 ~ 1.4 at a height of 4 m). Larger values of K_a are used at a multiplicity of air exchange equal to 3, smaller -10.

We inquired on authoritative websites about that the maximum allowable concentration of aluminum and alloys in the air is 2 mg/m^3 , substituting into the formula to calculate:

when supplying air with horizontal jets:

$$L = \frac{1000\beta V}{K_a C_{MAC}} = \frac{1000*1.6*0.044}{1*2} = 35.20 \text{ m}^3/\text{h};$$

when supplying to the working area:

$$L = \frac{1000\beta V}{K_3 C_{MAC}} = \frac{1000*1.6*0.044}{1.75*2} = 20.11 \ m^3/h.$$

4.4 Safety requirements in emergency situations

Types of hazards that may occur in the workplace include: fire; explosion (inside equipment, buildings or the environment); rupture or destruction of equipment; emissions of harmful substances; combination of these types of danger[50, 51]. In order to prevent the emergence and elimination of emergencies (emergencies) at the enterprise should be a plan for localization and elimination of emergencies and accidents in accordance with the provisions [52]. During the analysis of the danger of the enterprise (object) it is necessary to identify all possible emergencies and accidents, including unlikely, with catastrophic consequences that may occur at the enterprise, to consider scenarios for their development and assess the consequences. Identification of opportunities and conditions of accidents should be performed on the basis of analysis of features of individual equipment (devices, machines, etc.) and their group (technological units), as well as taking into account the hazardous properties of substances and materials (explosive and harmful) used in production. It is necessary to take into account the parameters of the state of substances (temperature, pressure, physical state, etc.) and the state of the equipment, which correspond to both the normal technological regime and the modes that are possible during the onset and development of the accident.

4.4.1 Fire safety

According to НАПБ Б.03.002-2007 [53], the laboratory has the characteristics of class B due to the presence of combustible objects (tables, cabinets, parquet floors, etc.). Primary fire suppression installations are designed to eliminate the center of a

small fire and to extinguish a fire in the initial stages of fire development by facility personnel before the arrival of dedicated firefighting units.

The main means of fire extinguishing include: fire extinguishers, fire extinguishing equipment (buckets, fire buckets, sandboxes, shovels, fire blankets) and fire extinguishing tools (hooks, crowbars, axes, etc.). Fire extinguishers and fire fighting equipment must be painted red.

The laboratory is equipped with a VVK-2 fire extinguisher. There is also a fire hydrant with a hose not far (15 m) from the laboratory.

Finding signs of fire in time and calling the fire brigade can quickly locate the fire source and take measures to eliminate the fire source, thereby greatly reducing the loss caused.

Electrical fire alarm systems (EPS) are considered the fastest and most reliable means of warning of a fire detectors are one of the main elements of an EPS installation.

DTL type thermal fire detectors are installed in the affiliated laboratory, the number is 4 sets. According to the detector square placement scheme, they are placed according to the specification.

The laboratory takes the following precautions:

1. Operators need to be familiar with fire safety content.

2. People who enter the laboratory should know the fire evacuation diagram.

3. Learn how to use fire extinguishers and their application scenarios in advance.

4. Daily fire detector maintenance and inspection.

4.4.2 Other safety

If there is a voltage failure in equipment such as scanning electron microscopes, optical microscopes or grinding machines, the circuit breakers on the switchboard must be turned off and the laboratory's chief engineer must be notified.

If someone gets an electric shock, it is necessary to disconnect the equipment available in the laboratory from the network, put the victim on the wooden floor, put

a cotton pad under the head, call 103 to call the doctor, and if necessary, conduct a medical examination on the victim. Artificial respiration.

If a fire occurs, it is necessary to turn off the circuit breaker and start extinguishing the fire with a fire extinguisher [54].

Every engineer or laboratory worker who discovers a fire or ignition must:

- Immediately call the University's 101 to notify the fire department;
- Start extinguishing the fire using the fire extinguishing tools available in the laboratory (fire extinguisher, fire hydrant, etc.);
-Call officials (Chief Engineer, Safety Supervisor, Superintendent) to the scene of the fire.

In case of injury, the chief engineer, the superintendent must be informed and go to the medical center [55].

CHAPTER 5. ECONOMIC SECTION

5.1 Scientific and technical relevance of the research topic

Lithium batteries are widely used in mobile phones, automobiles, notebook computers, portable devices, medical equipment, and weapon systems. Especially with the advent of the Internet era, people's demand for portable electrical appliances is increasing day by day. In particular, new energy represented by electric vehicles is impacting the status of traditional fuel vehicles. In addition, the demand for electric energy storage obtained from renewable energy and energy in the form of heat Also getting bigger and bigger.

Since the unique properties of nanomaterials can have beneficial effects on lithium batteries, the expansion of nanotechnology application fields requires in-depth study of these properties. Due to the very interesting physical properties of transition metal nanooxides, there has been an increased interest in the study of their structural features, properties, and electronic structural features.

Among the many unique properties of nanoscale oxides, their electrochemical properties are exploited to fabricate state-of-the-art adsorbent materials and cathodes for lithium current sources (LDS). Due to the defect structure of the nanoparticle surface and the characteristics of interatomic interactions, it is characterized by a large number of broken bonds and high surface energy. Since cations in oxides are surrounded by oxygen ions, the content of intercalated lithium ions mainly depends on their attraction to oxygen anions. Meanwhile, the content of adsorbents and intercalated Li ions is largely determined by their interactions with ions located on the defect surface of nanoparticles. The nature of this interaction depends on the charge states of these anions and the energy distribution of their valence electrons. Therefore, it is an urgent task to study the variation of valence electron energy distribution and ionic charge state with structural and dimensional features to improve the intercalation ability of materials.

5.2 Calculation of the planned cost of the research

The calculation of all the costs of the NDR related to the implementation of this topic makes it possible to establish the planned estimated cost of this topic. Planning ensures the reduction of labor and material costs in order to obtain the best results for the least costs.

Planned costs are determined from the following cost items:

1) Staff salary;

2) Social contribution;

3) Expenses for experimental materials;

4) Experimental equipment fee;

5) Third-party service fees;

6) Business trip expenses;

7) Other expenses not directly accounted for;

8) Indirect fees;

5.2.1 Calculation of staff salaries;

Fees under this clause include the salaries of all categories of employees performing the experimental work.

Wages are calculated based on labor intensity data for individual jobs and individual wages. Calculated in man-days. The list of jobs and their labor intensity are summarized in Table 5.1.

Table 5.1. Labor intensity of the stages of performing scientific and research work

Name of works on the research topic	Professor (days)	Research engineer (days)	Experiment executor (days)
Clarification and specification of tasks on the research topic	3	–	-
Formulate working methods	6	–	6
Equipment ready for experiment	2	8	11
Preparation of the mixture	2	6	10
X-ray structural analysis	2	8	12
X-ray Microspectroscopy	2	5	10
Result processing	5	2	20
Work product registration	3	–	6
Total workers	25	29	75

Multiply the daily average salary of each type of personnel by the corresponding planned labor intensity to calculate the planned salary fund for all personnel.

Daily wages are defined as the ratio of monthly wages to condition months (five-day work week).

The results of the calculation of personnel salaries on this topic are summarized in Table 5.2.

Table 5.2. Calculation of labor costs

Position of performers of the theme	Planned labor intensity, (days)	Salary, UAH		
		Monthly salary	Average daily salary	Total for workers

Professor	25	20507,09	970,29	24257.25
Research engineer	29	9238	435.75	3921.75
Experiment executor	75	-	-	-
Total labor costs in this work				28179

5.2.2 Determination of social contribution amount

The Single Social Contribution (SSC) is a compulsory contribution to national social insurance. From January 1, 2016, the SSC rate is 22%. The basis for the calculation of SSC are the total labor costs in this work. (summary of

).

Position of performers of the theme	Planned labor intensity, (days)	Salary, UAH		
		Monthly salary	Average daily salary	Total for workers
Professor	25	20507,09	970,29	24257.25
Research engineer	29	9238	435.75	3921.75
Experiment executor	75	-	-	-
Total labor costs in this work				28179

$$SSC = TC \cdot 0.22 \quad (5.1)$$

where TC - total labor costs in this work.

Currently, the SSC will be:

$SSC = 28179 \times 0.22 = 6199.38$ UAH.

5.2.3 Experimental Material Cost

Material cost is calculated based on the unit price and the total amount of material used. The calculation results are summarized in the Table. 5.3

Table 5.3. Experimental material price

Name of material	Unit	Mass	Market price per unit, UAH	Amount, UAH
Al_2O_3 powder (pure)	kg	2	540	1080
Fe_2O_3 powder (pure)	kg	0.5	414	207
Total				1287

We accept transport and procurement costs at the level of 10 % of the planned cost of total costs for materials:

$$C_M = T_C \times 1.1 \quad (5.2)$$

In this case, the total cost of purchasing materials and transporting them will be:

$C_M = 1287 \times 1.1 = 1415.7$ UAH

5.2.4 Experimental Equipment Cost

All work was performed on existing equipment and the cost of this article was not anticipated. A list of the equipment used is given in the Table. 5.4.

Table 5.4. List of scientific equipment required

The name of the equipment	Equipment model
Diffractometer	ДРОН УМ-1
Scanning electron microscope	Jeol JSM-6490LV, CamScan 4D
Microscope	Neophot 21
X-ray	Rigaku

5.2.5 The cost of third-party services

All work was carried out directly in the laboratories of the department of metallurgy and heat treatment, so there is no cost of third-party services.

5.2.6 Business trip expenses

All work is carried out directly in the laboratories of the Department of Metallurgy and Heat Treatment, so no travel expenses are provided.

5.2.7 Other direct unaccounted for expenses

This work combines all the costs of research work that are not included in the previous articles. When carrying out work, we accept other direct costs at the level of 10% of the amount of accrued costs for research work.

$$O_C = (TC + SSC + C_M) \cdot 0{,}1 \quad (5.3)$$

It will currently be:

$$O_C = (28179 + 6199.38 + 1415.7) \cdot 0{,}1 = 3579.41 \text{ UAH}$$

5.2.8 Indirect expenses

This work includes the costs associated with the management of the executing organization, the costs of invention and rationalization; depreciation costs of fixed assets; costs of scientific and technical information; costs of ensuring normal working conditions and safety; costs of paying for bank services; taxes, fees and other obligatory payments and expenses, etc.

Consider the option of calculating indirect costs in proportion to the amount of direct costs at the level of 20%.

$$I_C = (TC + SSC + C_M + O_C) \cdot 0{,}2 \quad (5.4)$$

It will currently be:

$$I_C = (28179 + 6199.38 + 1415.7 + 3579.41\ ) \cdot 0{,}2 = 7874.7 \text{ UAH}$$

5.2.9 Development of a planned calculation of the estimated cost of the work

The planned calculation of the cost of research in this work is based on the calculations and regulatory data (***Table*** able 5.5).

Table 5.5. Planned calculation of the estimated cost of research

Name of cost items	Amount, UAH	Rationale
Staff salary	28179	According to the calculations
Social contribution	6199.38	22.0% of total labor costs
Expenses for experimental materials	1415.7	According to the calculations
Experimental equipment expenses	–	According to the calculations
Third-party service expenses	–	No Third-party service fees
Business trip expenses	–	No business travel expenses
Other direct unaccounted costs	3579.41	10% of the amount of direct estimated costs in this work
Other expenses not directly accounted for	7874.7	According to the standards of the organization-executor of the topic (in our work 20% of the amount of direct costs)
Total	47248.19	Sum of all items

5.3 Scientific and technical efficiency of research

The calculation of the expected economic effect of research work is necessary to determine the feasibility of this work. However, it can be calculated only for of

research work, which is directly aimed at creating new materials, improving product quality parameters, as well as creating new designs.

To determine the annual economic effect, we use a scoring system to assess economic efficiency on the following indicators:

- the importance of development (K1);
- the possibility of using the results of development (K2);
- theoretical significance and level of novelty (K3);
- the complexity of the study (K4).

The total score (S) is calculated by multiplying the coefficients.

$$S = K_1 \cdot K_2 \cdot K_3 \cdot K_4 \quad (5.5)$$

In our case, the scoring of efficiency according to ***Table*** able 5.6 is:

$S = 3 \cdot 8 \cdot 3 \cdot 3 = 216$

Table 5.6. Score evaluation of the effectiveness of research

Research work performance evaluation indicator	Symbol of the indicator	Characteristics of this work	Scores
The importance of development	K_1	Work is performed under the agreement on scientific and technical cooperation	3
The possibility of using the results of development	K_2	The results of development can be used on the scale of one industry	8
Theoretical significance and level of novelty	K_3	During the work received new information that complements the idea of the essence of the studied processes	3
The complexity of the study	K_4	The work is performed by one unit, costs from 10,000 to 50,000 hryvnias	3

The conditional effect of research work is calculated by the formula:

$$E_{RW}^{C} = 500 \times S - E_N \times C_{RW} \quad (5.6)$$

where 500 is the notional value of one point;

E_N – normative coefficient of economic efficiency (can be in the range of 0.1 - 0.3);

C_{RW} – total costs of research work (RW) (Summary of Table 5.5);

In our work, the conditional effect of research work will be:

$E_{RW} = 500 \times 216 - 0.25 \times 47248.19$ =96187.95 UAH.

The economic efficiency of research is determined by the coefficient of conditional economic efficiency E_e.It is the ratio of the conditional effect of research work to the total cost of research work and is calculated by the formula:

$$E_e = \frac{E_{RW}}{C_{RW}} \quad (5.7)$$

In our work, E_e will be:

$$E_e = \frac{96187.95}{47248.19} = 2.04$$

The coefficient of conditional economic efficiency of research work is 2.045(>1), which indicates the feasibility of its implementation.

CHAPTER6. DEVELOPMENT STARTUP PROJECT

6.1 Description of the project idea

Lithium-ion batteries have attracted extensive attention as a driving force for electric vehicles due to their high energy density and power density. However, the anode materials of lithium-ion batteries commercialized at this stage are mainly graphite-based materials, and its theoretical specific capacity is only 372mAh g^{-1}, which cannot meet the needs of high-power and high-energy power batteries. Due to their special lithium storage mechanism, metal oxides generally have higher theoretical specific capacities (450mAh g^{-1} to 1500mAh g^{-1}) than graphite, and have broad application prospects. And metal oxidation is also a good catalyst.

Therefore, metal oxides have received extensive attention as anode materials. The reason why the metal oxide has such a high specific capacity is due to its special reaction mechanism: during the discharge process, the oxide reacts with metal lithium

to form lithium oxide and metal element. During the charging process, lithium oxide reacts with metal element to regenerate metal oxide and metal lithium.

The selection of metal oxides in a suitable state becomes the top priority, but the material volume of metal oxides will change greatly during the charge-discharge reaction, resulting in gradual pulverization of the material and loss of electrochemical activity. Therefore, the cycle performance of the lithium battery negative electrode material poor, which limits its commercial application.

The study found that the size of nano-materials is small, and the volume change of the material during charging and discharging is also small, which can effectively alleviate material pulverization and improve battery performance. Therefore, 80% Al_2O_3 and 20% Fe_2O_3 in nano-states are selected for research, which can be used in new lithium batteries in the future. widely used in batteries.

Table 6.1. Description of the idea of a startup project

Content of the idea	Directions of application	Benefits for the user
The relationship between the nanoscale 80% Al_2O_3/20% Fe_2O_3 mixture and the change of structure characteristics and capacity of lithium current source was studied.	Nanoscale 80% Al_2O_3/20% Fe_2O_3 Negative Lithium Current Source	More stable and larger capacity lithium battery

The comparative analysis of indicators is carried out: for the own idea the indicators having a) worse values (W, weak); b) similar values (N, neutral); c) the best values (S, strong).

Table 6.2. Identification of strong, weak and neutral characteristics of the project idea

№	Technical and economic characteristics of the idea	(potential) products / concepts of competitors			
		My project	Competitor1	Competitor2	Competitor 3
1	New technology	N	N	N	N
2	Excellent performance	S	N	W	N
3	Service life	S	W	W	N

6.2 Technological audit of the project idea

Within the limits of this division it is necessary to carry out audit of technology by means of which it is possible to realize the idea of the project (technology of creation of the goods).

Determining the technological feasibility of the project idea involves the analysis of the following components (Table 6.3):

Table 6.3. Technological feasibility of the project idea

Project idea	Technologies for its implementation	Technology availability	Availability of technologies
80% Al_2O_3 + 20% Fe_2O_3 nano powders	Vibration treatment (mechanical activation)	Available	Available
Selected technology for implementing the project idea: Vibration treatment (mechanical activation)			

The analysis of the results in the table shows that 80% Al_2O_3 + 20% Fe_2O_3 nano powder can be prepared by shock vibration treatment (mechanical activation).

6.3 Analysis of market opportunities to start a startup project

In the macroscopic world, the physical properties of the substance itself and the scale energy of the substance itself, so the nanometerization of the surface of the material is an inevitable trend of future development. Since the unique properties of nanomaterials can have a beneficial impact on lithium batteries, the expansion of nanotechnology application areas requires in-depth study of these properties. Due to the very interesting physical properties of transition metal nanooxides, there has been increasing interest in the study of their structural features, properties, and electronic structural features.

Among the many unique properties of nanoscale oxides, their electrochemical properties are exploited to create state-of-the-art adsorbent materials and cathodes for lithium current sources (LDS). Therefore, it is imperative to select a suitable nano-metal oxide to improve the capacity of lithium batteries.

Table 6.4. Preliminary description of the potential market of a startup project

№	Market indicators (name)	Characteristics
1	Number of main players, units	12
2	Total sales, RMB / （100 million）	17.6
3	Market dynamics (qualitative assessment)	Growing
4	Presence of entry restrictions (specify nature of restrictions)	No restrictions

5	Specific requirements for standardization and certification	1.High Purity Nano Powder 2. Can be used for lithium battery cathode
6	Average rate of return in the industry (or market), %	14.3

Compare the industry (or market) average rate of return with the bank's investment interest (3.78 %). The average rate of return in this industry is higher, so the investment in this industry makes sense.

According to the statistics, investigation and analysis of China Advanced Industry Research Institute of Lithium Battery, the consumption and total import and export scale of my country's lithium battery anode material market has been estimated. The total consumption scale of the Chinese market is on the rise. At the same time, the demand for nano-material lithium battery anodes in new energy vehicles, wind power, hydropower energy storage, portable appliances, military aerospace and other high-end fields is increasing, and it has excellent future application prospects.

Table 6.5. Characteristics of potential clients of the startup project

№	The need that shapes the market	Target audience (target market segments)	Differences in the behavior of different potential target customer groups	Consumer requirements for the product

1	Nano metal oxide lithium battery anode material	Lithium battery anode material	The market demand is high, and the supply may exceed the demand Affected by the development and research progress of lithium batteries and the global economy, the price is high	More stable and higher capacity lithium battery

After identifying potential groups of clients, the market environment is analyzed: tables of factors that contribute to the market implementation of the project and factors that hinder it are compiled . The factors in the table are presented in descending order of importance.

The Table 6.6 shows that threat factors.

Table 6.6. Threat factors

№	Factor	The content of the threat	The reaction of the company is possible
1	New competitor	Strong new competitors appearing to enter the market	Strengthen product technology innovation
2	Substitutes	Substitutes grab the company's sales	Strengthen product technology innovation

Table 6.7. Factors of opportunities

№	Factor	The content of the opportunities	The reaction of the company is possible

1	Market demand	Increase in market demand	Cooperate with other companies
2	new technology	New technology research	Technology transfer to new products to serve a larger customer base

Further analysis of the proposal is carried out: the general features of competition in the market are defined :

Table 6.5. Step analysis of competition in the market

Features of the competitive environment	What is this characteristic	Impact on the company's activities (possible actions of the company to be competitive)
Specify the type of competition - monopoly / oligopoly / monopolistic / pure	monopoly	Technology monopoly (independent research and development and production of products)
By level of competition - local / national /	local	Affect company performance
On a departmental basis between departments / industries	between industries	Research and development independent production line
Competition by types of goods:	freight-generic	Make the product apply to more fields
By the nature of competitive advantages - price / non-price	non-price	Improve product quality
By intensity - vintage / non-vintage	non-vintage	-

The final stage of the market analysis of project implementation opportunities is the compilation of SWOT-analysis (matrix of analysis of Strength and Weak, Threats and Opportunities).

The list of market threats and market opportunities is based on the analysis of threat factors and opportunities factors of the marketing environment. Market threats and market opportunities are the consequences (projected results) of the influence of factors, and, in contrast, are not yet realized in the market and have a certain probability of implementation.

Table 6.6. SWOT analysis of a startup project

S	Technical skill advantage: Tangible assets advantage; Human resources advantage.	W	Lack of competitive tangible assets, intangible assets, and organizational assets
O	Expanding trend of customer base or product segmentation; Strong market demand growth and rapid expansion; There is an opportunity to expand to other geographic regions and expand market share.	T	Strong new competitors appearing to enter the market; Substitutes grab the company's sales; Decline in the growth rate of the main product market; Adverse changes in exchange rates and foreign trade policies

6.4 Development of market strategy of the project

The development of a market strategy as a first step involves determining the strategy of market coverage: a description of target groups of potential consumers.

Table 6.7. Selection of target groups of potential consumers

№	Description of the profile of the	Readiness of consumers to	Estimated demand within	Intensity of competition	Easy to enter

	target group of potential customers	accept the product	the target group(segment)	in the segment	the segment
	There is a demand for large-capacity lithium batteries	Have confidence in the product and can accept it	High demand	The current market competition is not fierce, but increasingly fierce	Medium
Which target groups are selected:Automobiles, new energy, aerospace, electronics, military and other industries where large-capacity lithium batteries are widely used					

Based on the results of the analysis of potential consumer groups (segments), the authors of the idea choose the target groups for which they will offer their product and determine the market coverage strategy: it chooses a strategy of concentrated marketing;

To work in selected market segments it is necessary to form a basic development strategy.

6.5 Company development strategy

(1) Corporate mission: the leader in the lithium battery industry

The company focuses on the field of lithium batteries, serving lithium battery companies all over the world, improving production efficiency, improving product quality, and reducing production costs.

(2) Corporate vision: to become a world-class lithium battery related enterprise

Adhering to the spirit of "innovation is the primary productive force", the company has increased investment in scientific research, continuously carried out scientific and technological innovation, and strives to be in the forefront in the field of lithium batteries. Only continuous innovation will not be eliminated by rapid development and fierce competition. Excellent products, high technical content,

involving a wide range of technologies, for a wide range of customer groups. They are necessities and consumables in the field of modern new energy batteries. The market space is vast and the prospect is bright. We should continue to focus on this direction.

(3) Development strategy for the past 5-10 years

Becoming the world's top lithium battery company is our goal and dream for 20 to 30 years. In the past 5-10 years, after careful research and analysis, we have determined that our development strategy is "internationalization, intelligence, leanness, scale, and building a world-class lithium battery company"

6.6 Startups' Competitive Advantage

(1) Research and technical advantages

The company has outstanding independent research and development capabilities, attaches great importance to technical investment, and has a core team of professionals and operators with first-class theory and technology.

The company has high-end production equipment with independent intellectual property rights, which meets the special process requirements of nano-oxide lithium battery anode material products, greatly improves the quality of the company's products, firmly builds a higher technical barrier, and effectively improves production efficiency. Product cost provides performance and price advantages for companies to compete domestically and internationally.

(2) Product performance advantages

It can prepare and produce high-tech products, involve a wide range of technologies, and face a wide range of customer groups. It is a necessity and consumable for the modern new energy lithium battery industry.

(3) Advantages of prioritizing industrial development

At present, my country's lithium battery industry is in a climbing period. With the strong support of national policies, a huge market will be formed in the future. At the same time, it also belongs to the era of opportunities and challenges. Whoever can

seize the opportunity of technological innovation and walk at the forefront of the industry can stand firm, otherwise he will be eliminated.

6.7 Defining positioning strategy

(1) Target market positioning.

Lithium batteries using nano-oxide anodes have the characteristics of large capacity and stability. It is mainly used in new energy vehicles, electronic information, portable equipment and other industries, and the scope of application continues to expand. At present, all countries are vigorously developing the new energy industry, and there will be a broader application space in the future.

(2) Enterprise positioning (establishing enterprise brand).

The products a company sells are often closely related to its brand. The customer's recognition of your product actually starts with the recognition of the product brand. Brand positioning must be based on product positioning. It is achieved through product positioning, but once the brand positioning is successful, the brand as an intangible asset will be separated from the product and show its value independently. Through the implementation of brand strategy, the company has established a good brand system and established a good market reputation.

(3) Product positioning.

Product positioning is the positioning of a particular product in the minds of consumers. If consumers have similar needs, they will think of this brand's products. Because of their core technical capabilities and good product quality control, they are necessities and consumables in the new energy lithium battery industry, and have broad market space and prospects.

6.8 Development of a marketing program for a startup project

The first step is to form a marketing concept of the product that the consumer will receive.

The quality advantages of coated tools produced by start-ups are mainly reflected in the following aspects:

(1) Large battery capacity: A battery of the same size has a larger battery capacity.

(2) Good quality stability: Nano-scale metal oxides are used, the size of nano-materials is small, and the volume of the material changes during charging and discharging.

The pulverization of the material is also small, which can effectively alleviate the pulverization of the material and improve the performance of the battery:

The next step is to identify the best sales system for making the decision.

(1) First of all, we must know what the customer base is. Companies that apply to lithium battery related industries are potential customers. These customers can be contacted by company name, website and other means. This is very helpful for us to proceed to the next step. The collected information will be recorded, collated, analyzed, and prepared for the next step.

(2) Establish contact or relationship with customers

If salespeople want to sell products to customers, they must let customers know who you are, what company you are, what products you sell, and what products you have are advantageous. Therefore, whether it is a phone call or a visit from a stranger, these basic information must be clearly understood by customers. Our purpose is to help customers solve problems, help customers improve production efficiency, improve quality, provide technical support, thereby improving customer competitiveness, so as to sell our products, we must find people who are responsible for using or buying our products.

(3) Mining customer needs (arousing their desire to buy)

Analyze and digest the collected data. Analyze the customer's company organizational structure, from the customer's hierarchical functions and roles in procurement, find out customers related to procurement, straighten out the relationship, and find sales leads.

Compare the prices of similar products, the quality of the same price, the better the service, the higher the price and effect, and cost-effective. Find out what excites them about buying our products, so as to stimulate their desire to buy.

When customers have problems and challenges and need help, they ask if they want to buy a product or provide a service, and ask for it. Their underlying needs are their top priority. If we can solve problems on time, with quality, and according to their requirements, then doing business will not be a problem. The core of our sales is to solve the urgent needs of customers.

(4) Competitive strategy

Take advantage of price advantages, cost-effective advantages, technical advantages, after-sales service advantages, and relationship advantages. Adhere to the advantages and eliminate the disadvantages.

(5) Follow-up services

Monitor the arrival and subsequent use process, fulfill the after-sales service commitment, and ensure customer satisfaction. Establish a collection mechanism to ensure timely and volume collection of accounts. Continuously strengthen communication and understanding, continuously enhance mutual trust, and be a permanent customer. While letting customers introduce new customers to themselves, the customer base continued to expand.

6.9 Conclusions

National policies support the development of the new energy industry. As the most important part of new energy, the field of lithium batteries can drive the progress of the entire new energy industry. As an important core component of lithium batteries, anode materials can be said to play an important role in the overall performance of lithium batteries. A new nano-oxide material negative electrode can bring lithium batteries with greater capacity, thereby applying lithium batteries to a wider range of fields. Especially in the fields of new energy vehicles, new clean energy, portable equipment, aviation and military industry .These favorable policies and the general environment are conducive to the rapid development of enterprises in the industry, making startups commercially possible.

CONCLUSIONS

1. From the results of the SEM analysis, it was established that as a result of mechanoactivation of the 80% Al_2O_3+20% α-Fe_2O_3 mixture, the number and density of agglomerates, which consist of nanoparticles of aluminum and iron oxides, increase. From the results of TEM analysis, the injection of aluminum oxide particles into iron oxide particles was established.

2. From the results of X-ray diffraction, an increase in the size of the region of coherent expansion of Al_2O_3 and α-Fe_2O_3 in the mixture and a slight change in the phase composition of the nanocomposite due to processing were established.

3. A slight decrease in the intensity of the OKα and SiLα emission bands in the high-energy region, which occurs as a result of mechanoactivation, is a consequence of the mechanical penetration of harder Al_2O_3 nanoparticles into larger and softer α-Fe_2O_3 particles.

4. The charging capacity of the LPS with cathode based on the mechanoactivated mixture increases due to the injection of Al_2O_3 nanoparticles into α-Fe_2O_3 and the increase in surface defects of the nanoparticles of the mechanoactivated mixture.

REFERENCE LIST

1. Development of Preparation and Application of Alumina Nanopowder .HE Ke lan, LIN Jian, QIN Shuang .School of Materia ls Science and Engineering, Tong ji University, Shanghai 200092, China.

2. Ananthapadmanabhan P. V, et al. Formation of nano- sized alumina by in-fligh toxidation of aluminium powder in a therm al plasm a reactor [J]. Scripta Materialia, 2004, 50: 143- 147.

3. Ye R., et a l. In - fligh t spheroidization of alum in a powders in Ar- H2 and A r- N2 induction p lasmas [J]. Plasm a Chemistry and Plasm a Processing, 2004, 24 (4): 551 - 571.

4. The preparation and application nanometer-Al_2O_3.Li Hui yun, Zhang Tian sheng,Yang Nan. College of material Science and Chemical Engineering, Tianjin University of Science and Technology, Tianjin 300222, China.

5. Tang Bo, Ge Jie, Wang Chunxian, etc., New progress in the preparation of metal oxide nanomaterials [J], Progress in Chemical Industry., 2001, 21 (10): 707~712.

6. LuHongxia, SunHongwei.et, Materials Science and Engineering, 2005,42(10):406 -19

7. Zhang Yongcheng, Chen Shaou, Bulletin of Nano-Alumina Powder Silicate Prepared by Ammonium Bicarbonate Precipitation, 2007, 26(5): 23-27.

8. Liu Wei, Wu Xianxi, Chen Xiaohu, et al. Study on the preparation of ultra-fine aluminum hydroxide by alkoxide hydrolysis process [J]. Light Metals, 2004, 1: 11-13.

9. Chang Yufen, Shen Guoliang, Ning Gui Ling, et al. Preparation of polymorphic alumina nanoparticles in isopropanol system [J]. Chinese Journal of Materials Science and Engineering, 2004, 22 (2): 172- 174.

10. Thiruchitrambalama M, Palkarb V. R, Gop inathan c V. H ydrolysis of alumin ium metal and sol- gel processing of nano alumina[J]. Materials Letters, 2004, 58: 3063- 3066.

11. Chen Haiyang, Zhou Xichen, Xu Ming, et al. Preparation and

Characterization of Ultrafine Alumina [J]. Journal of Petroleum University, 2005, 29 (2): 116- 119.

12. Pathak L. C, Singh T. B, Das S, et al. Effect of pH on the combustion synthesis of nano- crystalline alum in a powder[J]. Materials Letters, 2002, 57: 380-385.

13. Hink lin T, Toury B, Gervais C, et a l. Liquid- feed flame spray pyrolysis of m etalloorganic and inorganic alumina sources in the production of nano alum in a powders [J]. C hem. Mater., 2004, 16: 21- 30.

14. Lu H. X, Sun H. W, Mao A. X, et a l. Preparation of plate-like nano - Al2O3 using nano-aluminum seeds by wet- chemical methods[J]. Materials Science and Engineering A, 2005, 406: 19-23.

15. Kamiya K, Hioki N, Hashimoto T, et al. Formation of A- alumina around 500□ in alkoxy - derived alumina gels under ambient pressure- effects of starting solution com position and seeding [J]. Journal of So l- Gel Science and Technology, 2001, 20: 275- 285.

16. Optical properties of a near-Σ11 a axis tilt grain boundary in α-Al_2O_3(Shang-Di Mo, W Y Ching and R H French.

17. Ru Qiang, Qiu Xiuli. First-principles calculations of the electronic structure and mechanical properties of Ot-A1O fJ1. Materials Research and Application, 2009 (3 162～167.

18. Zhong Hongmei, Yang Yanzhao, Zhang Weimin, et al 1 Study on the preparation of nano-iron oxide by reflux method Journal of Shandong University (Science Edition), 2002, 37 (2): 160-162.

19. Kandori K, Yasukawa A, Ishikawa T J1 Synthesis of uniform ferric oxide particle from deionized colloids. Colloid Interface Science, 1996 ,180 :446-452.

20. Sugimoto T, Sakata K, Muramatsu A J1 Hydrothermal synthesis and characterization of some polycrystalline α 2iron oxides. Colloid Interface Science ,1993 ,159 :372-382.

21. Cao Jianxin, Zhang Yu, Nie Dengpan. The latest progress in the

preparation technology of magnetic iron oxide nanoparticles [J]. Modern Machinery, 2003 (4): 80-82.

22. Jing Zhihong, Wang Yan, Wu Shihua. Hydrothermal Synthesis, Characterization and Magnetic Study of α-Fe_2O_3 Nano-powders with Different Morphologies [J]. Acta Inorganic Chemistry,2005,21(1):145-149.

23. Jing Su, Lu Xinning. Room temperature solid-phase synthesis of FeO-OH and Fe_2O_3 nanoparticles [J]. Journal of Nanjing University of Technology, 2002, 24(6): 52~ 54.

24. Grimm S, Schultz M, Barth S. Flam e pyro lysis - aprepa ration route for ultrafine pure- Fe_2O_3 powders and the control of their particle size and properties[J]. Materia ls Science, 1997, 32(4): 1080-1092.

25. A theoretical and experimental investigation of the electronic structure of α-Fe_2O_3 thin films Lidia Armelao, Marco Bettinelli, Maurizio Casarin, Gaetano Granozzi, Eugenio Tondello and Andrea Vittadini.

26. Research progress of iron oxide-based anode materials for lithium ion batteries,Tian Jiaming, Wang Jing, School of Materials Science, Hebei United University, Journal of Hebei North University, 2014.10.13-17.

27. Application of invention patent, Zhangjiagang, Dongwei New Material Technology Development Co., Ltd. Company, 201710816594.7

28. The latest research progress of metal/AI203 based nano composites. Zhang Aifei, Liu Jiping. School of Chemistry and Materials, Beijing Institute of Technology, Beijing 100081.

29. Вплив розміру наночастинок пірогенного кремнезему на енергетичний стан валентних електронів / Я.В. Зауличний, О.О. Фоя, В.М. Гунько та ін. // Фізика і хімія твердого тіла. – 2008. – Т. 9. – С. 767.

30. Енергетичний перерозподіл валентних електронів в анатазі TiO_2 внаслідок зменшення розмірів наночастинок / Я.В. Зауличний, О.О. Фоя, В.Л. Бекенєв та ін. // Наноструктурное материаловедение. – 2009. – №2. – С. 103.

31. Сканирующая электронная микроскопия как метод изучения микроскопических объектов электролитического происхождения / И.С.

Ясников, Ю.С. Нагорнов, И.В. Горбачев и др. // Физико-математические науки. – 2013. – № 1-3. – С. 758.

32. Зеер Г. М. Ледяева. Применение сканирующей электронной микроскопиив решении актуальных проблем материаловедения / Г. М. Зеер, О. Ю. Фоменко, О. Н. Ледяева // Journal of Siberian Federal University. Chemistry. – 2009. – № 4-2. – С. 287.

33. Оксидні електродні матеріали літієвих джерел струму / В.О. Коцюбинський, В.Л. Челядин, В.В. Мокляк та ін.. // Фізика і хімія твердого тіла. – 2010. – Т. 11, № 2. – С. 484.

34. Лазерна модифікація сполук інтеркалювання $Li_xTiS_2F_y$ / Б. К. Остафійчук, І.І. Григорчак, І. М. Будзуляк та ін. // Металофізика і новітні технології. – 2010. – Т. 32, № 6. – С. 749.

35. Зауличний Я. В. Зміна енергетичного розподілу валетних електронів при формуванні нанорозмірних сумішей SiO_2+Al_2O_3 пірогенним синтезом / Я.В. Зауличний, В.Я. Ільків, Ю.В. Яворський та ін. // Фізика і хімія твердого тіла. – 2015. – Т. 16, № 2. – С. 425-431.

36. Influence of Mechanical Treatment on Structural and Morphological Characteristics and Distribution of Valence Electrons of Aluminum, Silicon, Iron and Titanium Oxides / Yu.V. Yavorsky, Ya.V. Zaulichny, V.M. Gunko, M.V. Karpets// Journal Of Nano- And Electronic Physics – 2018. – Vol. 10 No 6, 06005(8pp).

37. Comparative study of electronic structures and dielectric properties of alumina polymorphs by first-principles methods / Choong-Ki Lee, Eunae Cho, Hyo-Sug Lee at al. // Physical review B. – 2007 . – Vol.76. – P. 245110.

38. Donatti D. A. Structural study of composites of aerosil fumed silica and tetraethoxysilane-derived sonogels / D.A. Donatti, A. Ibanez Ruiz, D.R. Vollet // Journal of Non-Crystalline Solids. – 2005. – Vol. 351. – P. 1226.

39. Брытов И.А. Рентгеноспектральное исследование электронного строения окислов кремния и алюминия / И.А. Брытов, Ю.Н. Ромащенко // Москва: ФТТ. – 1978. – Т.20, В. 3. – С.664.

40. Zaulychnyy Ya. V. Effect of mass ratio of initial precursors and mechanical

activation on distribution of valence electrons in Al_2O_3+Fe_2O_3 mixtures / Ya.V. Zaulychnyy, Y.V. Yavorskyi, V.I. Zarko at al. // Наноструктурное материаловедение. – 2015. – №1. – С. 4-12.

41. Гладкий Я. Н. Износостойкость детонационных покрытий системы $FeAl_2$-Ti-Si при нагружении трением в условиях повышенных температур / Я. Н. Гладкий, Е. Н. Лисовой // Проблеми трибології (Problems of tribology). – 2013. – Том. 68. – С. 82.

42. ДБН В.2.2-28-2010. Державні будівельні норми.

43. ДСН 3.3.6.042-99. Державні санітарні норми мікроклімату виробничих приміщень.

44. ДБН В.2.5-28-2006. Природне і штучне освітлення

45. ДСН 3.3.6.037-99. Санітарні норми виробничого шуму, ультразвуку та інфразвуку.

46. ПУЕ-2017. Правила улаштування електроустановок. – К.: Міненерговугілля України, 2017. – 617 с. НАПБ Б.03.002-2007

47. ДНАОП 0.00-1.21-98. Правила безпечної експлуатації електроустановок споживачів.

48. Местные вытяжные устройства к оборудованию для сварки и резки металлов: Методические указания по проектированию. - Л.: ВНИИОТ. – 1980. – 52 с.

49. ДБН В.2.5-67:2013. Опалення, вентиляція та кондиціонування.)

50. Положення щодо розробки планів локалізації та ліквідації аварійних ситуацій і аварій, № 424/3717 від 30.06.1999 р.

51. ДСТУ 3273-95. Безпечність промислових підприємств. Загальні положення та вимоги.

52. Y.-N. Xu, W.Y. Ching. Phys. Rev. B 44, 11 048 (1991).

53. ДСН 3.3.6.037-99. Санітарні норми виробничого шуму, ультразвуку та інфразвуку.

54. ДНАОП 0.00-1.21-98. Правила безпечної експлуатації електроустановок споживачів.

55. ДСТУ 3273-95. Безпечність промислових підприємств. Загальні положення та вимоги.